

Tactical Applications of Fluorine in Drug Design and Development

Nicholas A. Meanwell, Kyle J. Eastman, and Eric P. Gillis

Contents

1	Introduction	2
2	Fluorine and Conformation in Drug Design	4
2.1	Fluorine-Fluorine Interactions	5
2.2	Fluorine-Amide Interactions	7
2.3	Fluorine-Amine Interactions	12
2.4	Fluorine-Hydroxyl and Fluorine-Alkoxy Interactions	14
3	Modulation of pK_a with Fluorine	18
3.1	pK_a Trends with Fluorine Substitution	18
4	The Effect of Fluorine Atoms on Drug Potency	23
5	Effects of Fluorine on Metabolic Stability	28
6	The Effect of Fluorine Substitution on Membrane Permeability	31
6.1	Inter- and Intra-molecular H-Bonding of Fluorine	34
7	Fluorine in Positron Emitting Tomography (PET) Imaging	36
8	Conclusion	43
	References	44

Abstract The increasing utilization of fluorine in drug design parallels advances in understanding the physicochemical attributes of this element and an enhanced appreciation of how these unique properties can be exploited to address the numerous challenges encountered in pharmaceutical candidate optimization. Judicious placement of fluorine in a candidate compound can markedly affect potency, increase metabolic stability and enhance membrane permeability. The powerful electron-withdrawing nature of fluorine serves to modulate the pK_a of proximal functionality, particularly basic amines, and can be an important tool for controlling physical properties. Fluorine also exerts a conformation bias that is significant and can be utilized strategically. The ^{18}F isotope is of particular importance in positron

N.A. Meanwell (✉) • K.J. Eastman • E.P. Gillis
Department of Medicinal Chemistry, Bristol-Myers Squibb Research
and Development, 5 Research Parkway, Wallingford, CT 06492, USA
e-mail: Nicholas.Meanwell@bms.com; Kyle.Eastman@bms.com; Eric.Gillis@bms.com

emitting tomography (PET), an imaging technique of increasing importance for assessing drug-target engagement in both preclinical and clinical settings. This chapter provides a synopsis of some of the prominent and emerging applications of fluorine in the design and optimization of biologically active molecules.

Keywords *Gauche* interaction • Fluorine and basicity • Fluorine and conformation • Fluorine and hydrogen-bonding • Fluorine and membrane permeability • Fluorine and metabolic stability • Positron emitting tomography imaging

1 Introduction

Fluorine is a remarkable and unique atom capable of imparting a myriad of advantageous properties to small molecules, particularly in the context of medicinal chemistry. Over the last five decades the knowledge and understanding of this almost “magical” substituent has been enhanced substantially. Ever improving technologies for the installation of fluorine into novel small molecules facilitate attempts to utilize fluorine to address numerous challenges encountered in drug design: conformational control; modulating pK_a ; improving metabolic stability, solubility, permeability and potency; or tracking the distribution of a compound *in vivo* using positron emission tomography (PET) imaging. Recently, fluorine has found utility in fragment-based drug design by taking advantage of the ^{19}F NMR signal to both identify fragments that bind to targeted sites and to probe the presence of fluorophilic environments in proteins [1–3]. The applications of fluorine in medicinal chemistry continue to increase and its strategic deployment is considerably less empirical than it once was. However, there remains much to be understood regarding this privileged atom and its ability to aid in the fine tuning of pharmacodynamic (PD) and pharmacokinetic (PK) properties.

Fluorine is the most abundant halogen in the earth’s crust (and ranks 13th in abundance of all elements), but this has not translated into a proportional prevalence among naturally occurring organic compounds. There are only a handful of natural products known to contain fluorine, attributed to the fact that fluorine is found naturally in insoluble forms that are not readily available [4].

For example, seawater concentrations of fluoride have been measured at 1.3 ppm compared to ubiquitous chloride concentrations which are 1,900 ppm. Another factor contributing to the dearth of fluorine in organic molecules is the extremely high heat of hydration of fluoride [5]. Fluoride is heavily hydrated in water rendering it weakly nucleophilic and thus limiting its role in direct displacement chemistry. The high heat of hydration of fluoride relative to other halides is principally responsible for the inordinately high energy needed to generate F^+ from aqueous F^- [6]. This key difference from other halides precludes incorporation of fluorine into natural products *via* the haloperoxidase reaction that is a common pathway for the incorporation of chlorine, bromine and iodine [7, 8].

Despite the low concentrations of fluorine available on land and in the sea, some marine and terrestrial organisms can accumulate significant quantities of inorganic fluorine. However, the presence of organo-bound fluorine has only been identified in a

handful of tropical and sub-tropical terrestrial plants and in only two microorganisms. A great deal of effort has gone into the elucidation of the biosynthesis of fluorine-containing natural products [8–11]. The most prominent example is the synthesis of highly toxic fluoroacetic acid by the bacterium *Streptomyces cattleya* from *S*-adenosyl-L-methionine and fluoride mediated by the enzyme 5'-fluoro-5'-deoxy adenosine synthetase [9–11]. However, to date there is no evidence to support the *de novo* synthesis of the C-F bond in the animal or insect kingdoms [4]. Indeed, caterpillars of the moth *Sindus albimaculatus* acquire trifluoroacetate from their host plant, *Dichapetalum cymosum*, in concentrations that render them toxic to predators [12]. It is interesting that despite the scarcity of fluorine-containing compounds found in the natural world, fluorine plays a prominent and ever increasing role in contemporary drug design.

One of the earliest synthetic fluorinated drugs is 5-fluorouracil, an antimetabolite synthesized for the first time in 1957 (Fig. 1) [13]. Since that discovery, the

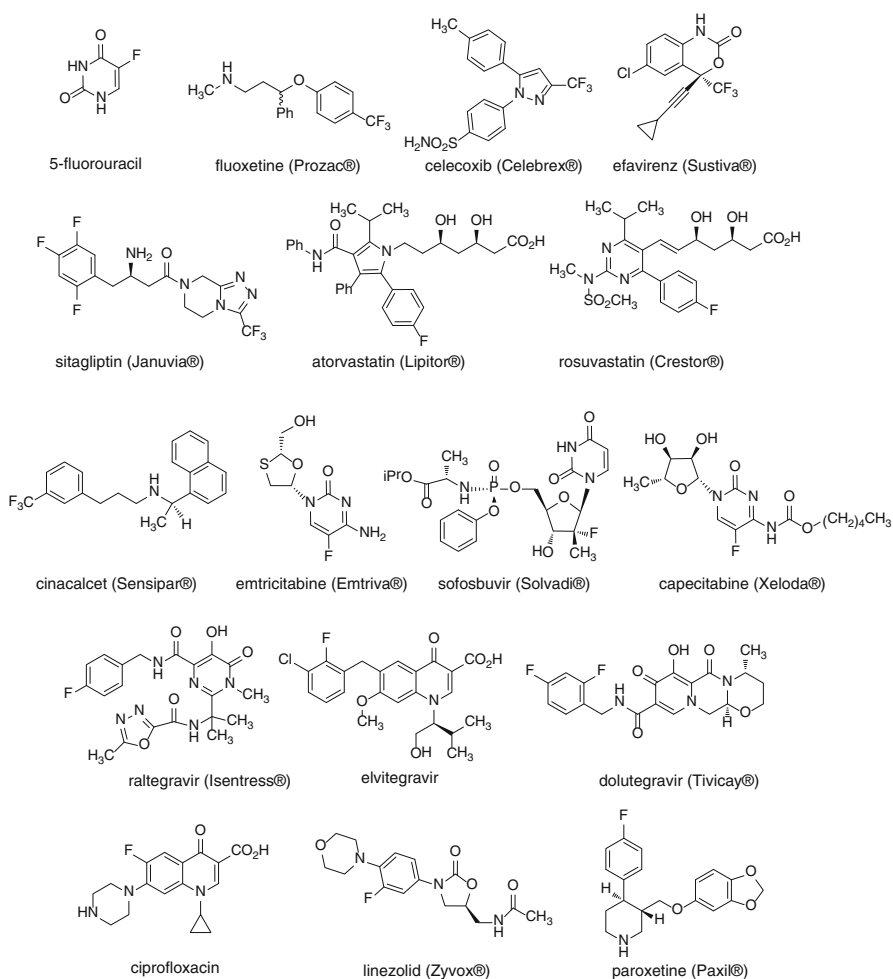


Fig. 1 (a, b) Examples of fluorine-containing drugs

deployment of fluorine in small molecule drug candidates has grown, as have the technologies to install this atom. Today, 20–25 % of marketed drugs contain fluorine, including blockbusters such as fluoxetine (Prozac®, depression), celecoxib (Celebrex®, arthritis), efavirenz (Sustiva®, human immunodeficiency virus (HIV)), sitagliptin (Januvia®, diabetes), atorvastatin (Lipitor®, dyslipidemia), rosuvastatin (Crestor®, dyslipidemia), cinacalcet (Sensipar®, hyperparathyroidism) and the nucleosides emtricitabine (Emtriva®, HIV). Other prominent fluorinated drugs include sofosbuvir (Solvadi®), capecitabine (Xeloda®, breast and colorectal cancer), the HIV integrase inhibitors raltegravir (Isentress®, HIV), elvitegravir (HIV) and dolutegravir (Tivicay®), ciprofloxacin, the prototypical fluoroquinolone antibiotic, linezolid (Zyvox®, antibiotic) and paroxetine (Paxil®, antidepressant). The objective of this chapter is to provide an overview of the impactful nature of fluorine on drug discovery as it is currently understood.

2 Fluorine and Conformation in Drug Design

The high electronegativity of fluorine is responsible for the strong polarization of the C-F bond, manifested as the highest measured dipole in organic molecules at 1.85 D for CH₃F. This phenomenon can strongly influence the interaction of C-F with a range of proximal functionality [14–22].

Depending on the nature of the functionality, these effects can be of sufficient magnitude to significantly affect conformational preferences, and can be exploited in the design of both drugs and organocatalysts [21, 22]. The basis for these intramolecular effects include dipole-dipole interactions, attractive electrostatic effects, repulsive effects between F and another electronegative atom, p-orbital repulsion, and a hyperconjugative effect in which the C-H bond of an adjacent atom interacts with the low lying σ^* orbital of the C-F bond [21–23]. An understanding of the interactive relationship between F and a range of organic functional groups has been developed using density functional theory (DFT) calculations that provide some instruction on potential utility and applications [23]. Table 1 captures the predicted energy of an individual interaction and offers a possible explanation for the preferred conformation based on the underlying physical chemistry [23]. Whilst several of these specific structural elements are of limited interest in drug design and the inherent energy of some interactions are too low to be of significance in the absence of additional reinforcing effects, the underlying physical organic chemistry principles offer considerable insight into the role that fluorine plays in influencing conformation. The most prominent functionality for which the energy of interaction with fluorine is such that the effect might be gainfully exploited in drug design are the amine, alcohol and amide moieties [21, 22].

Table 1 Calculated energy differences between the *gauche* and *anti* conformers of substituted fluoroethanes

R	Δ energy <i>gauche-anti</i> (kcal mol ⁻¹) B3LYP	Δ energy <i>gauche-anti</i> (kcal mol ⁻¹) M05-2X	Preferred conformer	Difference in dipole between the <i>gauche</i> and <i>anti</i> conformers (D)	Interaction underlying the predicted effect
-NH ₃ ⁺	-6.65	-7.37	Strongly <i>gauche</i>	NA	Electrostatic F δ^- and NH ₃ ⁺ δ^+
-NO ₂	-1.22	-1.12	Strongly <i>gauche</i>	4.42	Anti-parallel δ^- -FC-H and N δ^+ -O δ^- ; F δ^- and N
-NCHO	-1.00	-1.12	Strongly <i>gauche</i>	4.53	Electrostatic C-F δ^- and N-H δ^+
-F	-0.82	-0.66	Strongly <i>gauche</i>	3.02	σ C(F)-H to σ^* C-F
-N ₃	-0.76	-1.21	Strongly <i>gauche</i>	3.42	Electrostatic C-F δ^- and central N δ^+
-N=C=O	-0.74	-1.06	Strongly <i>gauche</i>	3.97	Electrostatic C-F δ^- and C=O C δ^+
-CH=NH	-0.25	-0.65	Strongly <i>gauche</i>	3.62	
-CH ₃	-0.18	-0.35	Weakly <i>gauche</i>	2.11	
-CH=CH ₂	-0.01	-0.17	Weakly <i>gauche</i>	1.95	
-C \equiv N	0.64	-0.64	Strongly <i>anti</i>	4.68	p orbital repulsion
-CHO	0.84	-1.20	Strongly <i>anti</i>	3.82	p orbital repulsion and anti-parallel dipole: C=O δ^- ... δ^+ HCF δ^-
-C \equiv CH	0.98	-1.03	Strongly <i>anti</i>	2.18	p orbital repulsion

2.1 Fluorine-Fluorine Interactions

The conformation of fluoroalkane derivatives is of considerable contemporary interest. The influence of fluorine on the conformation of vicinally substituted compounds is based on a stabilizing *gauche* interaction that relies upon hyperconjugation between a C-H bond and the low lying σ^* orbital of the C-F bond. The energy of this interaction is estimated to be 0.8 kcal mol⁻¹, modest but

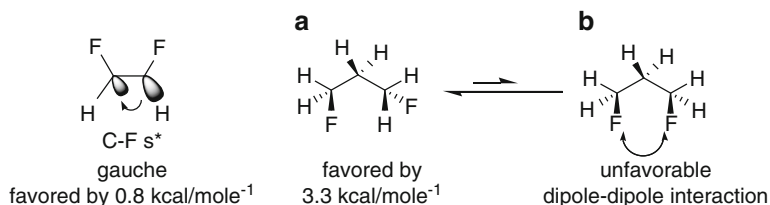


Fig. 2 (a) Conformation of 1,2-difluoroalkane, (b) conformational preference of 1,3-difluoropropane

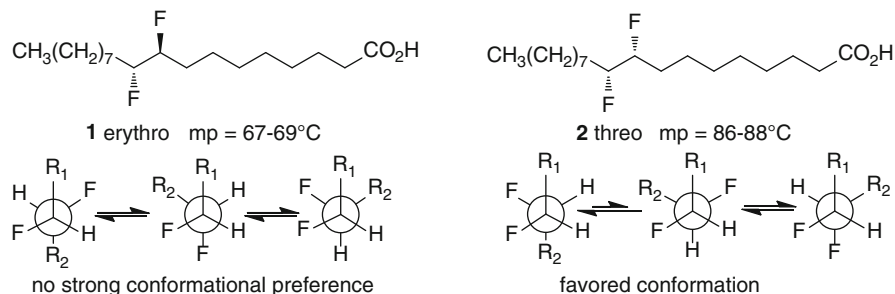


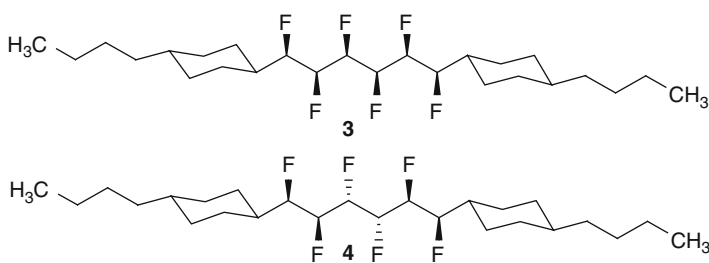
Fig. 3 *erythro*- and *threo*-9,10-difluorostearic acid **1** and **2** and Newman projections capturing their preferred conformations

nevertheless sufficient to exert an influence on conformation [21, 24] (Fig. 2a). In addition, there is a destabilizing repulsion between fluorine atoms in a 1,3-relationship that is of higher energy and which minimizes unfavorable dipole-dipole interactions [21, 24, 25]. The preferred conformation of 1,3-difluoropropane shown in Fig. 2b is estimated to be 3.3 kcal/mol⁻¹ more stable than the alternative [21, 24, 25].

An interesting example of the effect of the preference for a *gauche* arrangement of vicinal fluorine atoms on physical properties is provided by the two diastereomers of 9,10-difluorostearic acid, **1** (*erythro*) and **2** (*threo*), which were carefully synthesized in a fashion that ensured stereochemical integrity (Fig. 3) [24, 26]. These molecules differ only by the stereogenicity of the fluorine atom at C-10 yet their melting points differ by 20 °C, with the *erythro* isomer **1** melting at 67–69 °C while for *threo* isomer **2**, the melting point is 86–88 °C. The *threo* isomer **2** was anticipated to be the more stable isomer, with the fully extended form favored by the conformational preference exerted by the *gauche* interaction between the two F atoms, a conformation similar to that adopted by the native fatty acid. Langmuir isotherm measurements confirmed the similarity between **2** and stearic acid whilst the *erythro* isomer **1** displayed significant disorder, consistent with the lower melting point [24, 26]. In the Newman projections about the C9-C10 bond of **1**, the stabilizing effect of the *gauche*-disposed F atoms is offset by unfavorable

interactions between the two carbon chains such that none of the conformations are preferred although all are accessible.

Derivatives in which the vicinal difluoromethylene motif is extended to include 3, 4, 5 and 6 fluorine atoms have been examined to determine conformational preferences [24]. The most sophisticated study focused on the hexafluoromethylene motif, carefully assembled in the diastereomers **3** and **4**, that extended earlier studies on tetra- and pentafluoro alkanes [24, 27]. The conformation of these compounds, both in the solid state and in solution, indicates that in order to avoid unfavorable 1,3-dipolar interactions between F atoms, **3** adopts a helical topography that simultaneously allows the vicinal fluorine atoms to adopt the preferred *gauche* arrangement. The same effect favors an extended *anti* conformation for **4** that presents no unfavorable 1,3-dipolar interactions and facilitates 3 out of 5 possible *gauche* arrangements of the vicinal fluorine atoms [24, 27].



2.2 Fluorine-Amide Interactions

The conformation of α -fluoro-substituted amides is dominated by dipole-dipole interactions between the C-F and C=O bonds, with additional support from a productive electrostatic interaction between the fluorine atom and the amide NH if the molecule is configured appropriately [20, 28–33]. The synthesis and analysis of the enantiomers of α -fluoro capsaicin (**6**) as vanilloid receptor agonists is illustrative of the potential to take advantage of this kind of effect in drug design. *Ab initio* calculations of the rotational energy profile of 2-fluoro-*N*-methylpropanamide indicated that the *trans* conformer was the most stable with a 6 kcal mol⁻¹ advantage over the *gauche* conformer which was 2 kcal mol⁻¹ more stable than the *cis* conformer (Fig. 4) [28, 29, 33]. The stability of the *trans* conformation is attributed to a favorable alignment of the C-F and C=O bond dipoles supported by a productive electrostatic interaction between the F and amide H atoms. In the case of **6**, the (*R*) and (*S*)-enantiomers would be expected to adopt conformations that stereo-differentiated the side chain projection vectors, potentially providing insight into the bound conformation of the natural **5** [33].

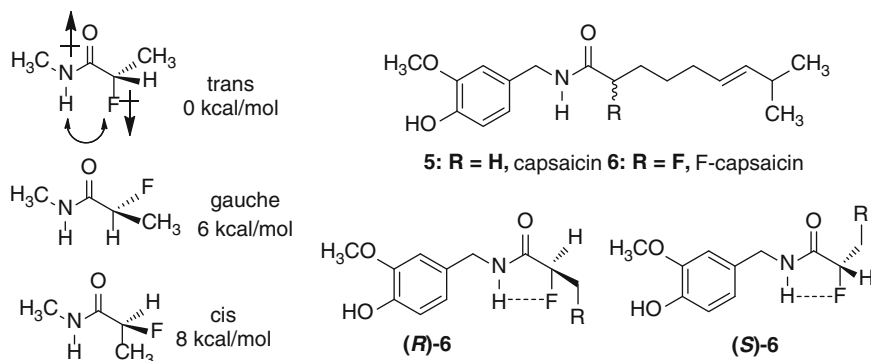
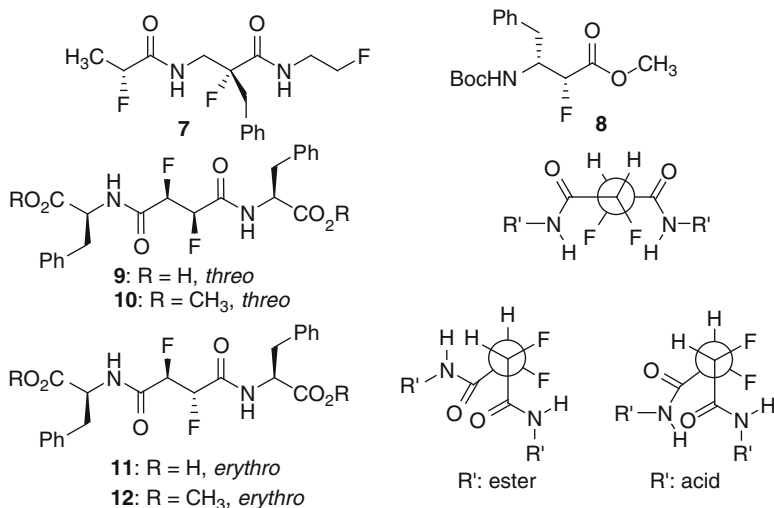


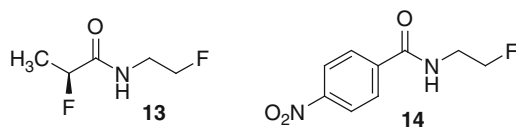
Fig. 4 *Ab initio* energies of conformers of *N*-methyl-2-fluoropropanamide. Potential conformation of (*R*) and (*S*)- α -fluoro capsaicin (**6**) at the TRPV1 receptor explored by these molecules

However, both the (*R*) and (*S*)-enantiomers of **6** performed similarly as TRPV1 receptor agonists, leading to the conclusion that the conformation captured by **5** in Fig. 4 in which the alkyl side chains project in vectors parallel to each other and in the plane defined by the amide moiety represents that of the natural product rather than that in which the alkyl chains project orthogonally to the plane of the amide, as depicted in (*R*)-**6** and (*S*)-**6** in Fig. 4 [33].

A study examining the effect of fluorination on the conformational preferences of β -peptide derivatives installed the fluorine atom α - to the amide carbonyl, a topology that simultaneously placed the F β - to the amine moiety. This structural arrangement allowed an analysis of the roles of the dipole-dipole effect between F and C=O and the *gauche* interaction between vicinally-deployed F and amide moieties [34]. X-ray crystallographic structures of the synthesized compounds revealed that the C-F and C=O bonds aligned in an *anti*-periplanar conformation to satisfy the dipole interactions whilst the F and amide moieties adopted the anticipated *gauche* arrangement [34, 35]. In the representative compound **7**, the torsion angle associated with the fluoropropionamide moiety in the solid state was -172.46° whilst that for the other α -fluoroamide was -179.7° . For the internal F-CH₂-CH₂-NHCO element, a torsion angle of -73.7° satisfied a *gauche* arrangement; however, in this particular example the F atom of the terminal NH-CH₂-CH₂-F moiety was disordered, interpreted as an effect of packing forces overcoming a *gauche* preference calculated to be $1.8 \text{ kcal mol}^{-1}$ [34, 35]. In the ester **8**, the torsion angle between the F atom and the ester C=O moiety was 154.5° , reflecting a reduced preference that is based on the weaker dipole associated with an ester that manifests as a calculated stabilization energy for the *anti*-periplanar form of $4.5 \text{ kcal mol}^{-1}$, which compares to $7.5 \text{ kcal mol}^{-1}$ for an α -fluoro amide and $2.2 \text{ kcal mol}^{-1}$ for an α -fluoro ketone [20, 28, 29, 35, 36].



The difluoro succinamide esters **9** (*threo*) and **11** (*erythro*) and the corresponding acids **10** (*threo*) and **12** (*erythro*) were prepared and the solid state structures determined which revealed conformational differences that were reflected in the preservation of a vicinal F-F *gauche* interaction in all 4 molecules [31, 32]. In the case of **11**, one of the fluorine-carbonyl pairs adopted a higher energy conformation that sacrificed the dipole-preferred *anti*-periplanar arrangement whilst in **9**, **10**, and **12** all arrangements between F and the C=O moieties were in, or very close, to the preferred *anti*-periplanar topography [31, 32]. NMR studies that analyzed $^3J_{\text{HF}}$ and $^3J_{\text{HH}}$ coupling constants revealed that these conformations were also prevalent in solution, underscoring the influence of the F-*gauche* effect.



The preference for a *gauche* relationship between fluorine and the N-CO moiety observed in **7** and **8** is of broader significance as a conformational tool. In the solid state, the conformation of 2-fluoro-*N*-(2-fluoroethyl)-propionamide (**13**) reflects a *gauche* relationship between the fluorine and NH-CO moieties, torsion angle = -69.9° , whilst the F atom α - to the amide carbonyl is aligned in a fashion consistent with the preferred dipole interactions in which the two are *anti*-periplanar, torsion angle = 2° [29]. A similar phenomenon is observed with **14** [35].

A particularly striking example of the *gauche* effect in β -fluoroamides is provided by the two 4-F proline diastereomers **15** and **16**. Here the fluorine atom exerts a significant influence on the conformational mobility of this unique amino acid, providing insight into the stabilizing influences of 4-hydroxyproline (**17**, Hyp), prevalent in the natural protein collagen [22]. Collagen is comprised of repeat units of Xaa-Yaa-Gly in which Xaa and Yaa are frequently proline or 4-(*R*)-Hyp. The polypeptide associates into a tightly-wound triple helix fibril, the thermal stability of which is enhanced by the presence of the hydroxyl substituent [37–42]. Although this phenomenon was initially attributed to the H-bonding properties of the hydroxyl moiety, a triple helix assembled from (Pro-4-(*R*)-F-Pro-Gly)₁₀ exhibits a CD spectrum identical to (Pro-Hyp-Gly)₁₀ or (Pro-Pro-Gly)₁₀ with all spectral data consistent with triple helix formation [37]. These observations support the conclusion that the stabilizing effect of Hyp (**17**) is based on an inductive effect rather than H-bonding. Following this observation, additional studies have evaluated the consequence of substituting the Xaa and Yaa positions with **15** and **16** rather than proline and Hyp (**17**), with the results leading to a deeper understanding of collagen conformation [38–43]. Proline has an inherent preference for the C γ -endo conformation, calculated as 0.41 kcal mol⁻¹, which favors this conformer by 2:1 at room temperature (Fig. 5) [44]. The introduction of a 4-(*S*)-F substituent (**16**) augments this preference, increasing the stability to a difference of 0.61 kcal mol⁻¹, stabilized by the *gauche* effect between the F and amide moieties that facilitates a conformation in which the F atom adopts an axial disposition (Fig. 5) [43, 44]. This effect is manifested in the single crystal X-ray of Boc-4-(*S*)-fluoroproline [43]. However, in 4-(*R*)-fluoroproline (**15**) the C γ -exo conformation is favored by 0.85 kcal mol⁻¹, stabilized by the *gauche* effect between the F and amide moieties that also disposes the F atom axially [44]. This phenomenon is mimicked by Hyp (**17**) where the C γ -exo conformer is calculated to be 0.48 kcal mol⁻¹ more stable than the C γ -endo conformer [45]. These insights provide an explanation for the structural similarity of (Pro-4-(*R*)-F-Pro-Gly)₁₀, (Pro-Hyp-Gly)₁₀ and (Pro-Pro-Gly)₁₀. Additionally, in **15–17** the E_{trans} isomer of the peptide bond is calculated to be more stable than the E_{cis} isomer regardless of the ring pucker, with the energy differences providing a stability hierarchy of 4-(*R*)-Pro > Pro > 4-(*S*)-Pro (Fig. 5) [38, 44]. The preference for an E_{trans} geometry has been attributed to this conformation allowing a favorable $n-\pi^*$ interaction between the O atom of the C=O moiety bound to the ring N atom and the C=O carbon of the exocyclic amide, as depicted in Fig. 5 [38, 46–48].

Molecular modeling studies have suggested that when proline is in the Xaa position of a (Pro-Pro-Gly)₁₀ helical strand, it adopts a C γ -endo pucker but when in the Yaa position a C γ -exo conformation is preferred, consistent with the observations noted above that (Pro-4-(*R*)-F-Pro-Gly)₁₀, (Pro-Hyp-Gly)₁₀ and (Pro-Pro-Gly)₁₀ form stable helical complexes [39, 49]. When a substituted proline is installed at the Xaa position, the conformational preference for the C γ -endo conformation would suggest that 4-(*S*)-F-Pro would function to form a collagen-like helix structure but the 4-(*R*)-F-Pro diastereomer would not based on their conformational bias [39, 43]. This has been observed experimentally with both

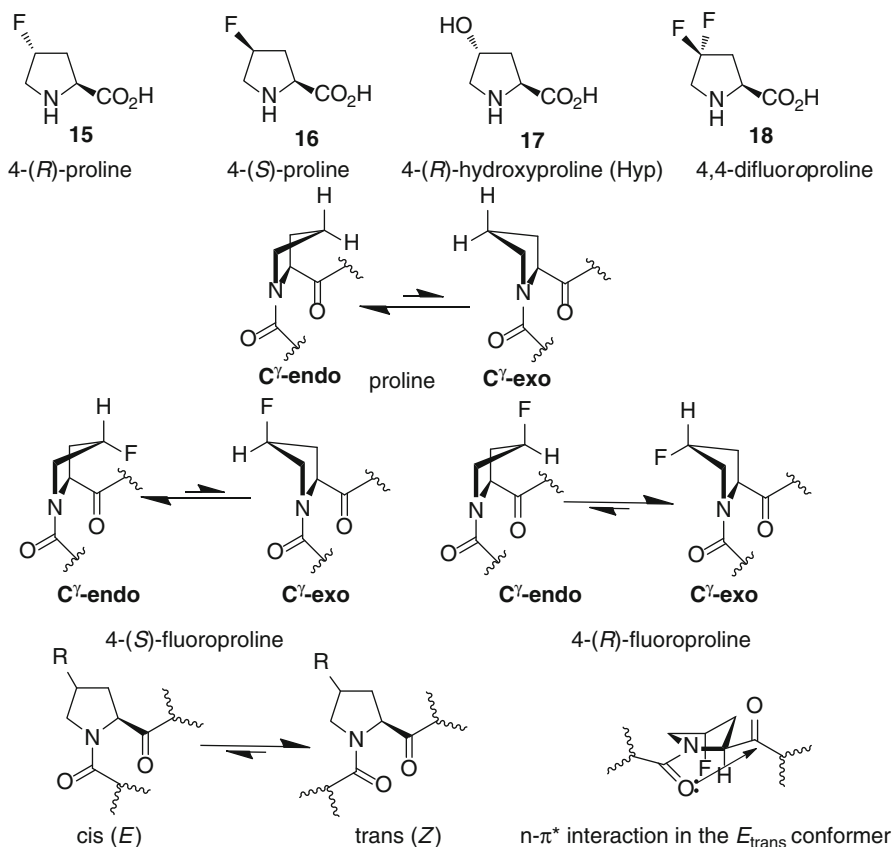
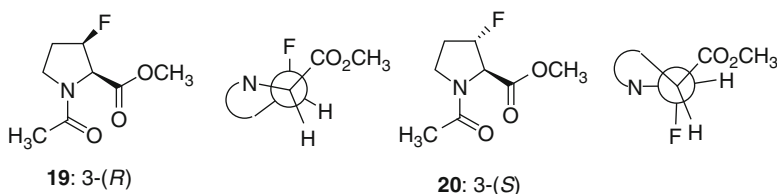


Fig. 5 Conformational preferences for proline, 4-(*S*)- and 4-(*R*)-fluoroproline. Preferred equilibrium for *cis-trans* amide isomerism in proline derivatives and stabilization of the *trans* isomer by a n to π^* interaction

(4-(*S*)-F-Pro-Pro-Gly)₁₀ and 4-(*S*)-F-Pro-Pro-Gly)₇, forming stable triple helices while (4-(*R*)-F-Pro-Pro-Gly)₁₀ and (4-(*R*)-F-Pro-Pro-Gly)₇ do not [39, 43]. Similarly, 4,4-difluoroproline (18), which offers no conformational bias, does not substitute effectively for Hyp (17) to form stable triple helices in collagen-related peptides [42].

Incorporation of fluorine at the 3-position of proline also introduces a conformational bias, a phenomenon initially explored with the diastereomeric esters 19 and 20 [50]. These molecules crystallized with the *trans* configuration between the amide and ester moieties, as depicted in 19 and 20, but the conformation of the proline rings differed, each stabilized by a *gauche* interaction between the F and amide moieties that deployed the halogen in an axial orientation. In 19, the pyrrolidine ring adopted the C^γ -exo conformation, which contrasts with 20 where the C^γ -endo

arrangement prevailed [50]. The stereoelectronic effects of the 3-F-prolines **19** and **20** are complementary to those of the 4-F isomers **15** and **16**. Thus, an *anti* orientation of the fluorine atom with respect to the ester moiety results in the *C γ -endo* conformation for **20** but a *C γ -exo* for **15** with the opposite effect for the *syn* epimers [50]. The *C γ -endo* conformation of **20** was found to be present in solution as assessed by the coupling constant between the α - and β -protons in the ^1H NMR spectrum. This coupling constant was ≤ 1 Hz and the calculated thermodynamic parameters suggested that this would be populated to the extent of 97 %. In contrast, the *C γ -exo* conformation of **19** was predicted to amount to 69 % of the population, attributed to repulsion between the F atom and adjacent ester moiety as a consequence of unfavorable steric and electronic interactions [41, 50]. The conformational preferences of **19** and **20** were preserved when these proline derivatives were incorporated into short peptide sequences [41, 50, 51].



2.3 Fluorine-Amine Interactions

Protonated β -amino fluoroalkanes show a strong preference to adopt a *gauche* conformation based on a favorable electrostatic interaction between the ammonium moiety and the electronegative F atom, the energetics of which are estimated to be 5.8 kcal/mol [20, 23, 52]. In the unprotonated form, 2-fluoroethylamine experiences only a weakly stabilizing intramolecular interaction between the NH_2 and F that has been viewed as a bridging H-bond estimated at ~ 1 kcal mol $^{-1}$ in favor of the *gauche* conformation, although the precise nature of fluorine-hydrogen interactions is controversial (*vide infra*).

In cyclic amines, such as the protonated form of 3-fluoro-*N*-methyl-piperidine (**21**), these interactions provide significant conformational bias [53–55]. In **21**, the ring F atom strongly prefers an axial disposition despite experiencing steric compression, with the calculated conformer populations provided in Fig. 6 [55]. As the global minimum, conformer A dominates to the extent of 95–96 %, stabilized by an electrostatic interaction between the F and NH^+ moieties, whilst conformer D contributes 4–5 % at equilibrium with the unfavorable diaxial interactions compensated by a productive electrostatic effect.

Trans-4-fluoro-*L*-proline (**15**) and its *cis*- isomer **16** both adopt a defined conformation in aqueous solution in which the favored conformations project the F atom in an axial orientation that is *gauche* with respect to the amino moiety [56].

Fig. 6 Conformational preference of **21** in its protonated form

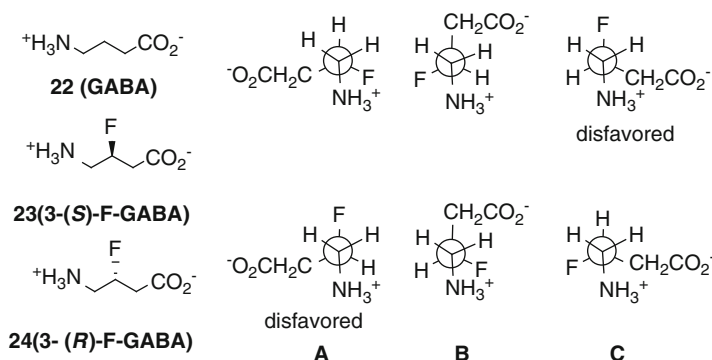
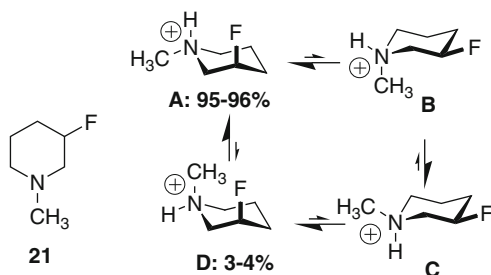


Fig. 7 GABA (**22**), the enantiomeric fluorinated derivatives **23** and **24** and their preferred conformations

The two fluorinated enantiomers **23** and **24** of the neurotransmitter γ -aminobutyric acid (GABA, **22**) represent an interesting example where the preferred *gauche* disposition between a protonated amine and a fluorine atom was used to glean insight into aspects of biologically-relevant conformations (Fig. 7) [57, 58]. The introduction of fluorine to GABA (**22**) reduces the basicity and increases the acidity of the natural amino acid in a fashion that preserves the zwitterionic nature at neutral pH. In solution, an extended conformation was observed for all molecules based on NMR analysis, stabilized in the case of **23** and **24** by the *gauche* interaction between the F and NH_3^+ moieties [57]. The range of conformations for each enantiomer are captured in Fig. 7 which also notes those that would be disfavored based on the absence of a *gauche* effect [57]. Both **23** and **24** were found to activate the cloned human GABA_A receptor with similar potency but were markedly less potent than GABA (**22**) itself [57, 58].

This observation suggested that the bound form of the neurotransmitter was the extended form accessible to both **23** and **24** in a fashion that preserves the *gauche* relationship between F and NH_3^+ , represented by conformation B in Fig. 7 [57, 58]. However, GABA aminotransferase caused elimination of HF from the (*R*)-isomer

24 with 20-fold higher efficiency than for the (*S*)-isomer **23**. This suggested that the conformation recognized by the enzyme placed the NH_3^+ and CH_2CO_2^- moieties in a *gauche* arrangement that would be destabilized, consistent with conformation C being preferred [57, 58] (Fig. 7). This conformation was also deduced to be that preferably recognized by the GABA_C receptor [59]. Both **23** and **24** were found to act as agonists rather than antagonists at $\rho 1$ and $\rho 2$ GABA_C receptors, with the (*R*)-isomer **24** the more potent but still ten-fold weaker than GABA (**22**), whilst the (*S*)-isomer **23** was 20-fold weaker than the natural ligand, attributed to weaker electrostatic interactions as a consequence of the reduced basicity. These observations suggested that GABA (**22**) adopted a folded binding orientation represented by conformation C at the GABA_C receptor [59].

An analogous strategy was adopted to probe the bound conformation of *N*-methyl-D-aspartate (**26**), an agonist of the neurotransmitter glutamic acid (**25**), at recombinant GluN2A and GluN2B receptors expressed in *Xenopus laevis* oocytes (Fig. 8) [60]. (2*S*,3*S*)-3F-NMDA (**27**) was prepared in an enantiospecific fashion whilst (2*S*,3*R*)-3F-NMDA (**28**) was obtained along with the (2*R*,3*S*)- stereoisomer after separation of diastereomeric α -methylbenzylamine precursors. Analysis of ^1H - and ^{19}F NMR spectra indicated distinct chemical shifts and coupling constants for the individual compounds that were consistent with (2*S*,3*S*)-3F-NMDA (**27**) in solution adopting conformation A, shown in Fig. 8, whilst (2*S*,3*R*)-3F-NMDA (**28**) avoided conformer C and was concluded based on DFT calculations to prefer conformer B, the conformer observed in the single crystal X-ray structure. In the biological assays, (2*S*,3*S*)-3F-NMDA (**27**) evoked currents in oocytes expressing either GluN2A or GluN2B receptors, although the responses were less than that observed with NMDA (**26**), whilst (2*S*,3*R*)-3F-NMDA (**28**) and its enantiomer were essentially inactive [60]. These results suggested that only (2*S*,3*S*)-3F-NMDA (**27**) was able to adopt a conformation similar to that of bound NMDA (**26**), designated as A in Fig. 8. This result is consistent with X-ray crystallographic data of NMDA (**26**) bound to the GluN2D receptor which is highly homologous to the GluN2A and GluN2B receptors.

The effect of a fluorine atom β - to a protonated amine on conformational preference and its potential impact on biological recognition has further been documented in 8-membered rings and in fluorinated pyrrolidine elements incorporated to replace the peripheral pyrrolidines of G-quadruplex binding ligands based on an acridine scaffold [61, 62].

2.4 Fluorine-Hydroxyl and Fluorine-Alkoxy Interactions

The *gauche* conformation of β -fluoroethanol derivatives has been estimated to be favored by ~ 2 kcal mol $^{-1}$ when the F and OH moieties can engage in an intramolecular H-bonding-like interaction [52, 63, 64]. In the absence of this interaction, the preference for the *gauche* relationship is essentially absent, with an energy

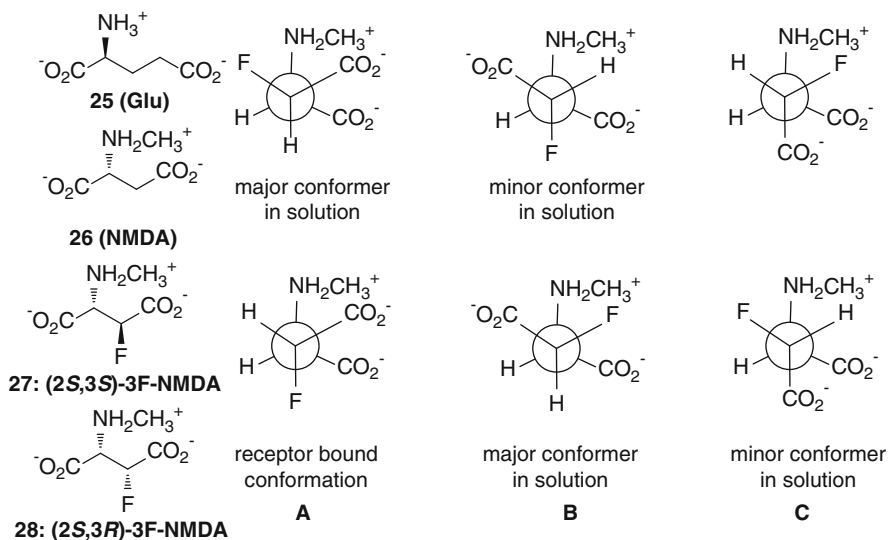
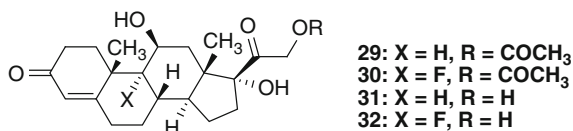
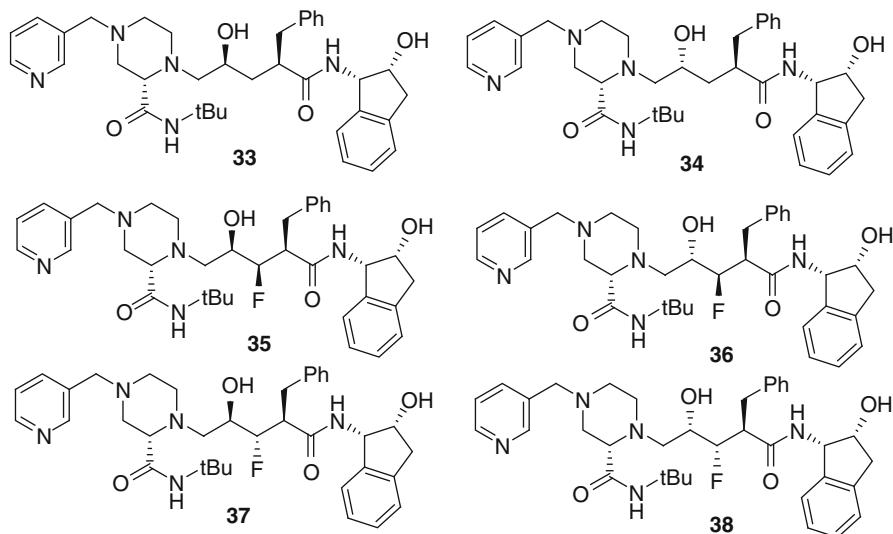


Fig. 8 Structures of glutamic acid (**25**) NMDA (**26**), the enantiomeric fluorinated derivatives **27** and **28** and their preferred conformations

estimated at only 0.1–0.2 kcal mol⁻¹. However, protonation of the alcohol significantly enhances the stability of the *gauche* conformer, estimated at ~7 kcal mol⁻¹ and attributed to a combination of both a stereoelectronic effect and an intramolecular HO-F interaction [52, 63, 64]. Several drug design studies have attempted to exploit the effects of deploying F and OH moieties in a vicinal arrangement that either take advantage of the *gauche* conformational preference or the effect of F on the H-bonding potential of the hydroxyl. An early example explored the effect of replacing the C-9 α -H atom of hydrocortisone acetate (**29**) with F to afford **30**, which demonstrated ten-fold greater glucocorticoid activity in restoring liver glycogen deposition in the adrenalectomized rat and four- to nine-fold higher activity at increasing the survival time of adrenalectomized dogs with a concomitant reduction in sodium retention [65, 66]. Fludrocortisone (**32**) is an anti-inflammatory agent that improved on the therapeutic index of the progenitor hydrocortisone (**31**) and was the first marketed fluorinated pharmaceutical product [67]. The origin of the improved biological properties of fluorinated steroids remains enigmatic and may be a function of the combination of several effects that includes the increased acidity of the 11 β -hydroxyl moiety, a distortion of the A ring due to non-bonded interactions between the F atom and proximal axial substituents and reduced metabolism *in vivo* [14, 68–70].



The judicious introduction of a fluorine atom into the HIV-1 protease inhibitor indinavir (**33**) and epi-indinavir (**34**) provided an opportunity to assess the effect of F-OH interactions on biological properties related to conformational disposition [71]. The four fluorinated derivatives **35–38** were prepared with the anticipation of complex effects due to the F atom which was expected to affect the acidity of the OH and influence the population of conformers in addition to affecting steric interactions and solvation. The K_i data for the inhibition of HIV-1 protease are summarized in Table 2 and reveal interesting profiles.

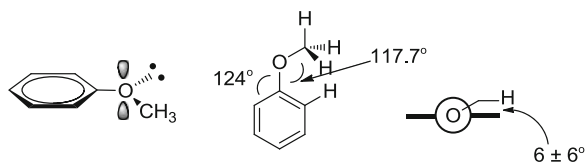


The syn, syn fluorinated derivative **35** fully retained the activity of the parent drug **33** while the anti,anti isomer **37** was an order of magnitude weaker. For the epi-indinavir derivatives **36** and **38**, the syn,anti analogue **38** improved potency by eight-fold over **34** whilst the anti,syn diastereomer exhibited a 36-fold weaker K_i [71]. An analysis of the ^1H - ^1H and ^1H - ^{19}F coupling constants indicated that the syn,syn (**35**) and syn,anti (**38**) diastereomers adopted the fully extended conformation that characterizes indinavir (**33**) when bound to HIV-1 protease, attributed to

Table 2 K_i data of **33–38** for the inhibition of HIV-1 protease

Compound	K_i (nM)	Log P	Compound	K_i (nM)	Log P
33	1.9	3.03	36	5,900	3.31
34	160	3.02	37	27	3.01
35	2.0	3.23	38	20	3.12

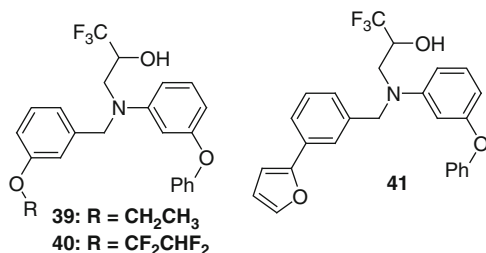
Fig. 9 Conformation of arylmethyl ethers



the preference of F and OH to adopt a gauche relationship. In contrast, the other 2 diastereomers **36** and **37** populated additional conformers to a significant extent, providing an explanation for the observed reductions in potency. The lipophilicity of each of the diastereomers was determined from the measured 1-octanol/water partition coefficient and all were marginally increased compared to indinavir (**33**), with the exception of the anti,anti analogue **37**.

Fluorination also impinges on the conformation of ethers, most prominently in anisoles [15, 72–74]. Arylmethyl ethers without *ortho* substituents adopt a conformation in which the methoxy moiety is close to coplanar with the aryl ring, a consequence of rehybridization of the substituent that maximizes electronic overlap of the oxygen atom with the π system and overcomes the inherent allylic 1,3-strain, with bond angles summarized in Fig. 9 [75–79]. In contrast, the trifluoromethoxy substituent is typically orthogonal to the plane of the benzene ring, favored by 0.5 kcal mol⁻¹, inverting the calculated 3 kcal mol⁻¹ preference for planarity observed with anisole [15, 80]. Difluoroalkoxyaryl moieties behave similarly, indicating that these structural elements should not be considered as simple isosteres of alkoxy substituents but as moieties capable of exploring a broader range of conformational space [15, 74].

The arylethyl ether **39** is an inhibitor of cholesterol ester transfer protein, IC₅₀=1.6 μ M, but the fluorinated homologue **40** is eight-fold more potent, IC₅₀=0.2 μ M, attributed to a combination of steric effects and drug-protein interactions that are more favorable in **40** [73].



Ab initio calculations indicated that while the ethoxy moiety preferred a conformation coplanar with the aryl ring, the fluorinated ether projected in a vector that was more perpendicular. Interestingly, a 2-furyl substituent provided the optimal OCF₂CHF₂ mimetic, IC₅₀=0.48 μ M, attributed to the preferred conformation of the furan ring also being orthogonal to the plane of the phenyl moiety [73].

3 Modulation of pK_a with Fluorine

Fluorine is the most electronegative element (Pauling electronegativity of 3.98) [84]. Due to the significant electron-withdrawing influence that fluorine exerts inductively through σ -bonds, fluorine substituents typically lower the pK_a of neighboring functionality (although exceptions exist [81]): protic groups become more acidic as measured by a decrease in the pK_a of the functional group itself, and basic groups become less basic as measured by a decrease in the pK_a of the conjugate acid. The ionization state of basic and acidic functionality not only affects potency and the absorption, distribution, metabolism, and excretion (ADME) properties of a molecule, but may also play a role in reducing the potential for a compound to exhibit toxicity [82]. Specifically, molecules incorporating basic nitrogen atoms are known to be more promiscuous and may show increased potential for cardiovascular toxicity *via* promoting interference with the hERG potassium ion channel and may increase the occurrence of phospholipidosis [83–86]. The significant influence of fluorine on the pK_a of adjacent functionality, in combination with other desirable properties including a small steric volume (similar in volume to oxygen) and high metabolic stability of the C-F bond, provides a powerful tool by which to modulate pK_a during drug candidate optimization [14].

3.1 pK_a Trends with Fluorine Substitution

An understanding of the correlation between fluorine substitution and pK_a enables a rational approach to drug candidate optimization. For acyclic aliphatic amines, the observed pK_a often represents the contribution of a conformational average of substituents and, as a consequence, the decrease in pK_a due to fluorine substitution is generally additive [87]. As shown in Fig. 10, the shift in pK_a of aliphatic amines due to fluorine substitution can be accurately predicted based on this additive property. The significance of the effect decreases with increased σ -transmission distance: each fluorine substituent at the β -carbon reduces the pK_a by 1.7 units, at the γ -carbon by 0.7, and at the δ -carbon by 0.3. As a point of reference for the calculation, the pK_a of alkyl amines can be generally approximated as primary amine = 10.7; secondary amine = 11.1; and tertiary amine = 10.9 [87, 88]. The chain length of the alkyl groups does not generally shift the pK_a of the amine; however, *N*-methyl substitution is an exception (Fig. 11) [87].

For unstrained cyclic amines in saturated systems the change in pK_a upon substitution can be approximated by summing the contribution of both σ -transmission pathways [87, 88]. Figure 12 demonstrates the application of this approach towards a series of substituted piperidines. For example, in 3-fluoropiperidine there are two σ -transmission pathways from the fluorine atom to the nitrogen atom: “path

<i>n</i>	Prediction ΔpK_a	Experimental pK_a			
		<i>y</i> =0	<i>y</i> =1	<i>y</i> =2	<i>y</i> =3
1	-1.7	10.7	9.0	7.3	5.7
2	-0.7		9.9		8.7
3	-0.3	10.7			9.7
4	-0.1				

Fig. 10 For aliphatic amines, the change in pK_a due to fluorine substitution is generally additive in nature [88]

 10.7	 11.1	 10.9	 8.0	 11.3	 11.3
 10.7	 10.9	 10.2	 11.1	 11.1	
 10.6	 10.9	 10.5	 7.9	 10.3	 10.1
		 9.8			

Fig. 11 pK_a values of acyclic and cyclic alkyl amines [88, 89]

predicted	σ -path 1	$\gamma = -0.7$	$\delta = -0.3$	$\gamma = -1.4$	$\delta = -0.6$	
	σ -path 2	$\gamma = -0.7$	$\beta = -1.7$	$\gamma = -1.4$	$\beta = -3.4$	
	ΔpK_a	-1.4	-2.0	-2.8	-4.0	
observed	pK_a	11.1	9.4	9.3	8.5	7.4
	ΔpK_a		-1.7	-1.8	-2.6	-3.7

Fig. 12 Predicted and observed pK_a of fluoro-substituted piperidines [88]

1”=F-C-C-C-C-NH and “path 2”=F-C-C-NH. The pK_a of 3-fluoropiperidine can therefore be predicted using the values of the linear system provided in Fig. 10: $pK_a = 11.1$ (piperidine) $- 0.3$ (“path 1”) $- 1.7$ (“path 2”) = 9.1. This predicted value is in close agreement with the experimental pK_a of 9.3.

Fig. 13 Dipole minimization of the N⁺-H and C-F bond leads to stabilization of the protonated amine

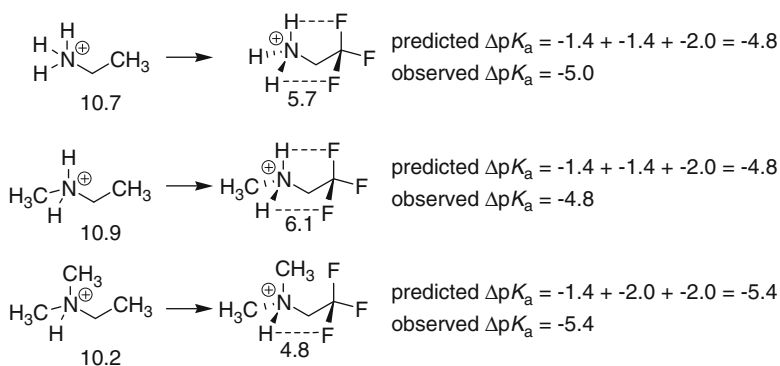
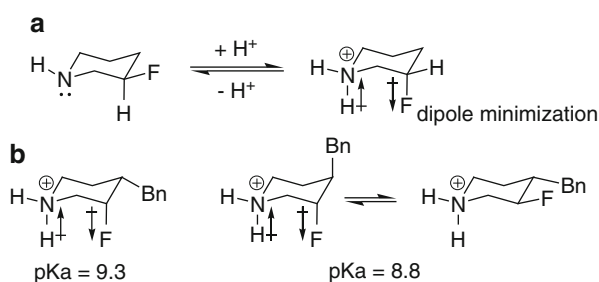


Fig. 14 The *syn*- β -fluoro effect can be used to refine $\text{p}K_a$ predictions for amines containing β -fluoro substitution [88]

That the observed $\text{p}K_a$ of 3-fluoropiperidine is slightly less acidic than predicted may be explained by stabilization of the ammonium species *via* dipole minimization, as depicted in Fig. 13a [88]. In fact, NMR studies with 3-fluoropiperidine have revealed that the 3-fluoro substituent inverts from a completely equatorial orientation to a completely axial orientation upon protonation of the amine [53]. Similarly, the fluoro substituent of *cis*-3-fluoro-4-benzylpiperidine adopts a completely axial orientation in the protonated species leading to stabilization and a $\text{p}K_a$ of 9.3 (Fig. 13b). Upon protonation of *trans*-3-fluoro-4-benzylpiperidine, the 3-fluoro substituent occupies both the axial and equatorial orientation equally, leading to reduced stabilization and a $\text{p}K_a$ of 8.8 [88].

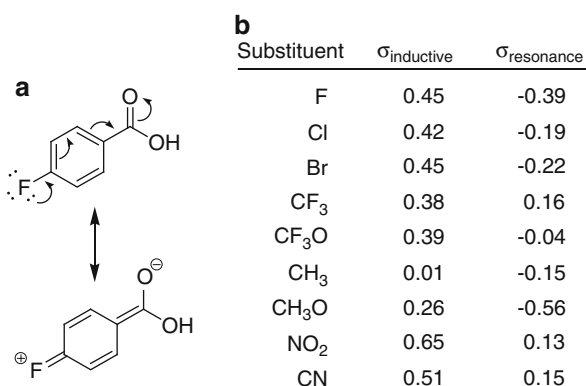
The stabilization of ammonium species *via* *syn*- β -fluoro substituents appears to be a general phenomenon. The $\Delta\text{p}K_a$ shift due to β -fluoro substitution can be refined to accommodate for this influence: $\Delta\text{p}K_a = -1.4$ for a full 1,3-*syn* CF⁻NH⁺ interaction and $\Delta\text{p}K_a = -2.0$ in the complete absence of a 1,3-*syn* CF⁻NH⁺ interaction [88]. This refinement enables the accurate prediction of $\text{p}K_a$ values for primary, secondary and tertiary amines with β -fluoro substituents (Fig. 14).

Table 3 Experimental pK_a measurements from a series of methanesulfonamides demonstrate an additive change in pK_a upon fluorine substitution [90]

n	R=H	R=Ph	R=3-C ₆ H ₄ COPh
0	10.8	8.85	8.19 ^a
1	9.32 ^a	7.57 ^a	6.77 ^a
2	8.06 ^a	6.19 ^a	5.44 ^a
3	6.33	4.45	3.70 ^a

^aaqueous pK_a values were calculated from experimental measurements obtained with solvent = 67% DMF-H₂O

Fig. 15 (a) Fluorine is inductively electron-withdrawing but is electron-donating through resonance. (b) The discrete inductive contribution and resonance contribution to Hammett's σ_{para} constants [14]

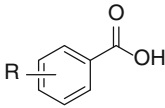
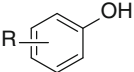


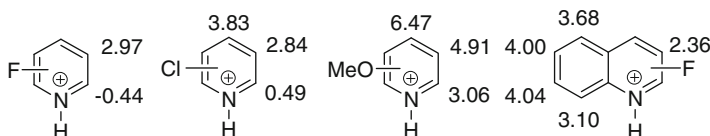
Additionally, the *syn*- β -fluoro effect may, in part, account for the difficulty in predicting the pK_a of imperfectly staggered heterocycles such as fluoro-substituted pyrrolidines [88].

Fluorine substitution of methanesulfonamides also leads to an additive decrease in the pK_a of the NH proton. As shown in Table 3, the decrease in pK_a is approximately 1.47 units per fluorine substituent and is independent of the R-group bound to nitrogen [90]. The linearity observed in this trend is postulated to be due to the small steric changes associated with replacing hydrogen by fluorine and the fact that fluorine substitution is somewhat remote (two atoms away from the acidic site) [90]. In the case of fluoroacetic acids, the decrease in pK_a due to fluorine substitution is not additive: the pK_a of acetic acid=4.76; fluoroacetic acid=2.59; difluoroacetic acid=1.33; and trifluoroacetic acid=0.50 [91].

Although fluorine exerts a strong electron-withdrawing influence through σ -bonds, fluorine is electron-donating through resonance (Fig. 15a). Due to the excellent 2p orbital overlap between fluorine and carbon, this influence can be quite strong and the significance of this effect is not matched by the other halogens (Fig. 15b) [14, 92]. Due to these opposing forces, the effect of fluorine on pK_a in

Table 4 pK_a values of benzoic acids and phenols [91, 94]

Substituent						
	pK_a^{ortho}	pK_a^{meta}	pK_a^{para}	pK_a^{ortho}	pK_a^{meta}	pK_a^{para}
H	4.02	4.02	4.02	9.99	9.99	9.99
F	3.27	3.87	4.14	8.73	9.29	9.89
Cl	2.88	3.83	3.99	8.55	9.10	9.43
Br	2.85	3.81	3.99	8.45	9.03	9.34
F ₃ C	4.0	3.6	3.6	8.3	9.0	8.7
H ₃ C	3.90	4.27	4.36	10.3	10.0	10.3
H ₃ CO	4.09	4.08	4.49	9.99	9.65	10.2
NO ₂	2.18	3.46	3.44	7.22	8.35	7.15

**Fig. 16** pK_a values of mono-substituted fluoro pyridines and quinolines (pK_a pyridine=5.17; pK_a quinoline=4.85). pK_a values of analogous chloro and methoxy pyridines are provided for comparison [17]

aromatic systems is strongly dependent on the through-resonance relationship of the fluorine substituent and the functional group of interest. Fluorine acts as an electron-withdrawing group in positions *ortho*- or *meta*- to functionality. Fluorine in a *para*-relationship to a functional group behaves as a neutral substituent because the through-resonance electron-donating character of fluorine essentially cancels out its inductive electron-withdrawing influence [92]. As shown in Table 4, this trend is observed with benzoic acids and phenols, archetypal systems of cross-conjugated and directly-bound functionality, respectively. Similarly, the changes in pK_a of aniline ($pK_a=4.62$) upon fluorine substitution is: 2-fluoroaniline= -1.40 , 3-fluoroaniline= -1.04 and 4-fluoroaniline= $+0.03$ [17]. Basic heterocycles such as pyridine also follow this trend (Fig. 16). Although the aqueous pK_a of 4-fluoropyridine has not been reported, gas phase measurements indicate that 4-fluoro substitution leads to a small decrease in the pK_a in the gas phase and a predicted aqueous pK_a similar to that of pyridine [93]. It should be noted that the CF₃ group is electron-withdrawing both inductively and through-resonance, and thus always reduces the pK_a of adjacent functionality [93, 94].

4 The Effect of Fluorine Atoms on Drug Potency

Appropriate modulation of pK_a , conformational preference, hydrophobic interaction, hydrogen bonding, lipophilicity, solubility or a combination of these properties exerted by the deployment of fluorine atoms can improve potency/binding affinity and sometimes even selectivity of drug molecules. This phenomenon is manifested in many examples taken from a wide range of areas of medicinal chemistry.

In keeping with the theme from the previous section, the influence of fluorine on the pK_a of basic functionality was systematically studied in the context of optimizing the pharmaceutical properties of a thrombin inhibitor [95]. All permutations of single and double fluorine substitution of the amidinium-bearing arene were synthesized and the pK_a of the amino group of the tricyclic skeleton (pK_{a1}) and the pK_a of the amidinium residue (pK_{a2}) were experimentally determined (Fig. 17). The change in pK_a upon introduction of fluorine followed the expected trends, with the exception of double fluorine substitution *meta*- to the amidinium group, compound **45**. In this case, the pK_a unexpectedly increased to 4.21 from 4.10 measured for the mono-fluoro analog **44** and insight into this phenomenon was sought through DFT calculations (RB3LYP, 6-31G**). For the mono-fluorinated arene, the *exo*-conformer, which minimizes allylic-1,3-like strain between the nitrogen lone pair and fluorine, is calculated to be 3.4 kcal mol⁻¹ more stable than the *endo*-conformer (Fig. 18a). In the difluorinated arene, unfavorable allylic strain is unavoidable, as illustrated in Fig. 18b. Upon protonation, both the mono- and di-fluorinated arenes adopt conformations in which there is a favorable C-F...H-N⁺ interaction. However, because this favorable interaction is present in both analogs, the increased basicity of the difluoro analog is best explained by the differences observed in the unprotonated state,

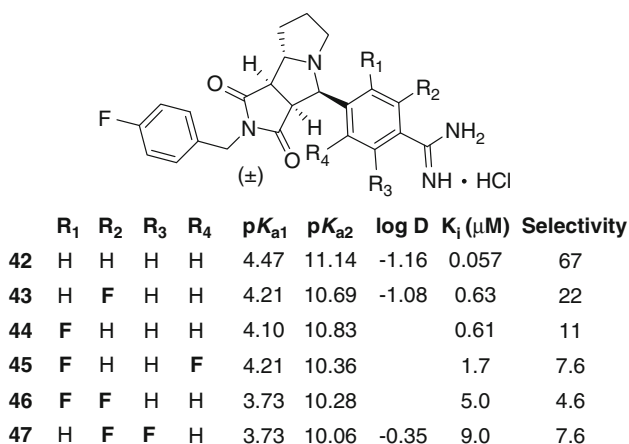


Fig. 17 Properties of a series of thrombin inhibitors: the pK_a of the amino group of the tricyclic skeleton (pK_{a1}), the pK_a of the amidinium residue (pK_{a2}), log D, binding affinity (K_i), and selectivity for thrombin compared to trypsin as a function of fluorine substitution [95]

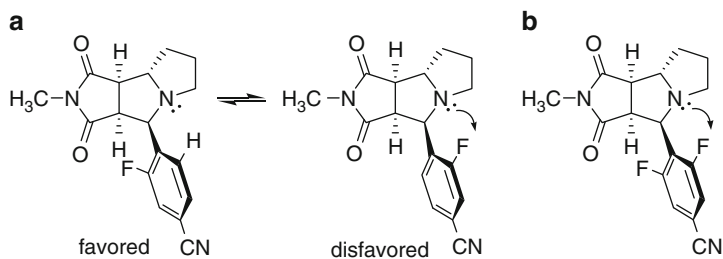
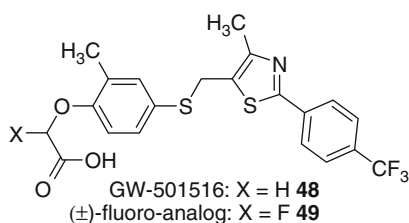


Fig. 18 (a) Allylic 1,3-like strain between the fluorine and the nitrogen lone pair disfavors the *endo*-conformation of the mono-fluorinated arene. (b) For the di-fluorinated arene, proximation of the nitrogen and fluorine atoms is unavoidable



Compound	EC ₅₀ (nM)	PPAR α EC ₅₀ (nM)	PPAR γ EC ₅₀ (nM)	PPAR δ EC ₅₀ (nM)
48	0.03	>1000	912	2.9
49	3.7	560	>1000	55

Fig. 19 Activation of oleic acid oxidation (EC₅₀) and agonism of individual PPAR subtypes by acids **48** and **49** [97]

i.e., the electrostatic interaction between the C-F dipole and the nitrogen lone pair [91]. In all cases the decrease in pK_a corresponded to a decrease in binding affinity (K_i). Although the change in binding affinity is likely complex in origin, linear free energy relationships correlating pK_a and binding free enthalpies ($-\Delta G$) calculated for inhibition of thrombin and trypsin demonstrated a relationship between affinity and pK_a . Specifically, this analysis found that inhibition of thrombin is 2.5 times more sensitive to the pK_a of the amidine functionality than is inhibition of trypsin, providing a possible means towards increasing thrombin selectivity [95].

Peroxisome proliferator-activated receptors α , δ and γ (PPAR α , PPAR δ and PPAR γ) are implicated in regulating transcription of genes responsible for lipid and carbohydrate metabolism [96]. A series of fluorine-substituted analogs of the PPAR δ modulator GW-501516 (**48**) was synthesized and studied based on the hypothesis that fluorine substitution at the α -carbon (**49**) would reduce the pK_a of the adjacent carboxylic acid moiety and lead to stronger binding affinity (Fig. 19) [97]. In practice, the fluoro-substituted analog **49** was a less potent activator of oleic acid oxidation than the progenitor GW-501516 (**48**). However, when the affinity of

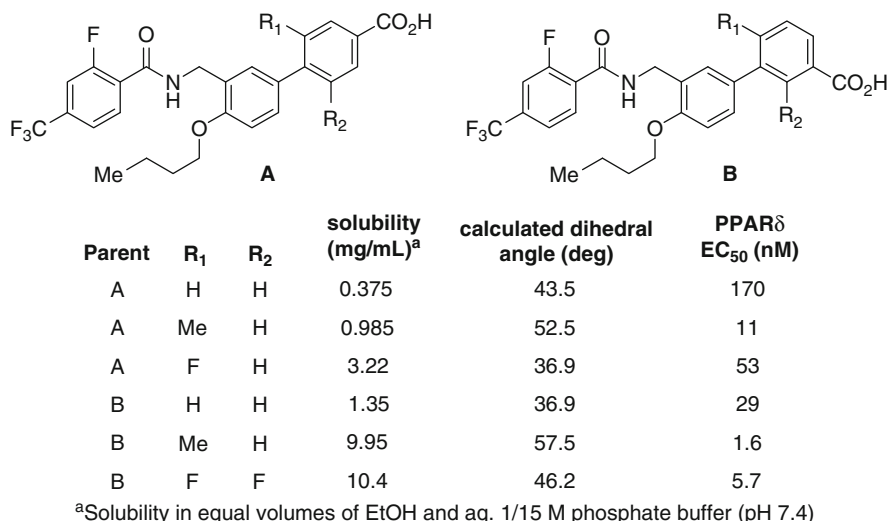
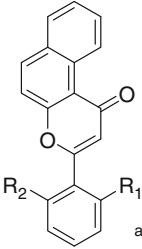


Fig. 20 The solubility, calculated dihedral angle, and EC₅₀ values for a series of PPAR δ agonists [98]

each compound towards the PPAR subtypes was assayed, it was found that the fluoro-analog demonstrated a modestly positive effect on PPAR α activation, essentially behaving as a modest dual PPAR α/δ agonist. Computational modeling predicted that both enantiomers of the fluoro-analog bound similarly, and that the dual agonism is due to interactions remote from the fluorine atom.

Judicious fluorine substitution can provide a means of improving the solubility of drug molecules. The solubility of several classes of pharmaceutical compounds can be improved by disrupting molecular planarity and, in turn, potentially reduce crystal packing density [98]. Although this argument explains, in part, the observed improvements in solubility, fluorine substitution leading to increased solubility is explained “not only by disrupting molecular planarity but also *via* other mechanism(s)” [98]. In these cases, the trends observed in Fig. 20 can be understood as a manifestation of the inductively withdrawing/resonance-donating electronic effects of fluorine that underlie its influence on pK_a. For example, fluorine substitution *ortho* and *meta* to a carboxylic acids leads to an increase in acidity which can consequently increase solubility. Fluorine is a strong through-resonance donor (*vide supra*) which can impart partial π -bond character to biphenyl systems, leading to a decrease in dihedral angle, but this effect is reduced if there is a strong resonance-accepting group such as a carboxylic acid *ortho* or *para* to a fluorine atom.

This through-resonance effect of a fluorine atom is also manifested in the properties observed with the series of fluorine-substituted aryl hydrocarbon receptor (AhR) agonists depicted in Fig. 21 [98]. The decrease in dihedral angle is most dramatic for the mono-fluoro analog **51** where solubility is increased. Both of these changes are likely due to an increase in polarization resulting from strong through-resonance communication between the fluorine substituent and the ketone

	R ₁	R ₂	solubility (mg/mL) ^a	calculated dihedral angle (deg)	EROD EC ₅₀ (μM) ^b	
	50	H	H	84.6	17.8	1.4
	51	F	H	153	9.1	0.33
	52	F	F	248	40.5	0.20
	53	H	Me	262	37.9	>10
	54	Me	Me	1270	70.0	>10

^aSolubility in equal volumes of EtOH and aq. 1/15M phosphate buffer (pH 7.4).
^b7-ethoxyresorufin *O*-deethylase (EROD) activity in MCF-7 breast cancer cells.

Fig. 21 The solubility, calculated dihedral angle, and EC₅₀ values for a series of AhR agonists [98]

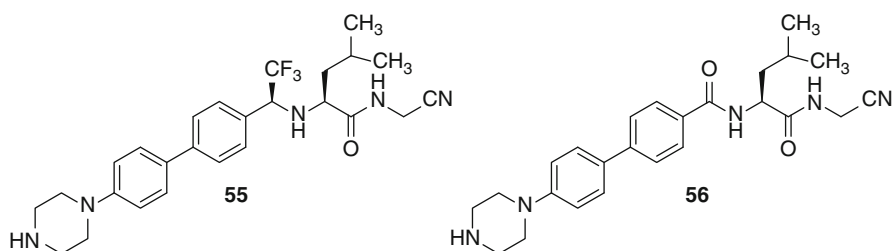


Fig. 22 Cathepsin K inhibitors

functionality. In the case of the difluoro derivative **52**, both the dihedral angle and solubility are similar to the mono-methyl substituted compound **53**, suggesting that disrupting planarity may be the underlying influence. Fortuitously, fluorine substitution also led to an increase in potency as well as solubility.

An example of fluorine substitution in the context of the cysteine protease cathepsin K highlights not only the advantageous impact of fluorine on potency but also the isosteric relationship between a trifluoroethylamine moiety and an amide [99]. The replacement of amide bonds with isosteric functionality has been extensively explored within the field of medicinal chemistry and there are many well-established isosteres of the amide moiety. However, there are only a few isosteres that conserve the hydrogen-bond donating properties of the amide. Reduction of an amide to the corresponding amine not only removes a hydrogen-bond acceptor but also introduces a basic amine, typically providing poor mimetic properties. Addressing this deficiency, the strategic introduction of a trifluoromethyl moiety led to reduced basicity whilst preserving the near 120° backbone angle and conferring isopolarity with the carbonyl moiety, as illustrated by **55** in Fig. 22 [99, 100]. In addition to providing an acceptable isostere for the bis-amide **56**, trifluoroethylamine **55** also exhibited improved potency and selectivity compared to **56**. The trifluoroethylamine derivative **55** was the most potent compound identified, demonstrating an IC₅₀ of less than 0.005 nM toward inhibition of cathepsin K. Modeling

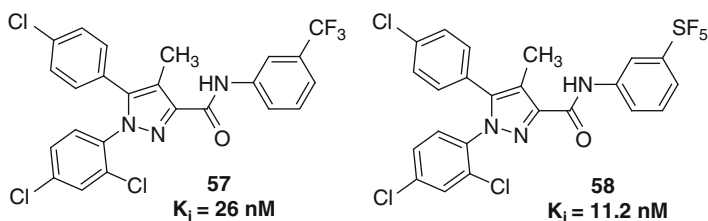


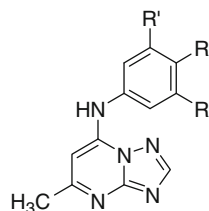
Fig. 23 Cannabinoid CB₁ receptor ligands

and SAR were used to rationalize the stark difference in potency between **55** and **56** [99]. Specifically, in **55** the sp² nature of the amide leads to an interaction with the adjacent aromatic ring which enforces a suboptimal geometry for both the aromatic ring and for the hydrogen-bonding interaction to the protease. In the case of **55**, the newly introduced sp³ center allows for a perpendicular arrangement of the aromatic ring thus stabilizing it in what is presumed to be the active conformation while simultaneously allowing for a more optimal hydrogen bond interaction with a residue in the active site. In addition to improved potency and selectivity with **55**, the metabolic stability was also increased significantly: **55** demonstrated no susceptibility toward hydrolysis, a significant liability observed with dipeptide compounds.

The SF₅ substituent has not been extensively exploited in drug design despite that this group has been referred to as a “super trifluoromethyl group” due to the fact that these two functionalities share many features (although this designation is probably imprecise) [101–104]. The shared features between SF₅ and CF₃ include high electronegativity, good thermal and chemical stability and high lipophilicity, with the SF₅ group exhibiting each of these features to a greater extent than the CF₃ group. Both of these substituents are xenobiotic and have remarkable stability under physiological conditions, lending to their usefulness in drug discovery. While there is some consensus on CF₃ being similar in size (van der Waals volume) to the ethyl group, comparative comments on the relative size of an SF₅ moiety are more speculative [16]. However, it has been suggested that the volume of the SF₅ group is slightly less than that of a *tert*-butyl group but larger than the CF₃ group [102]. In addition to differences in size, the geometries of these two groups are quite different. The SF₅ group displays a pyramid of electron density whereas the CF₃ group is associated with a cone shape of electron density [103]. The subtle differences in properties between these two groups provides opportunity for deployment of the SF₅ group in a fashion that allows optimization of many of the PK and PD properties discussed in this chapter, including potency. An interesting example where an SF₅ moiety provided an advantageous impact on potency is in the context of cannabinoid CB₁ receptor ligands [104]. In two different pyrazole series illustrated by the prototype *meta*-CF₃-aniline **57** and its SF₅ analogue **58** (Fig. 23), the SF₅ compounds consistently exhibited a lower K_i for the CB₁ receptor than the CF₃-analogs. The increased potency was attributed to a potential “better fit” of the SF₅ group in a pocket of the CB₁ receptor relative to the CF₃ group, indicating that in this setting the two groups are not biologically equivalent.

Table 5 SAR associated with a series of *Pf*DHODH inhibitors

	R	R'	IC ₅₀ (uM)	
			<i>Pf</i> DHODH	<i>Pb</i> DHODH
59	SF ₅	H	0.13	0.38
60	CF ₃	H	0.28	0.28
61	CF ₃	F	0.19	0.11



Another example where SF₅ and CF₃ substitution has been examined in a matched pairs-type of analysis was disclosed in the context of a *P. falciparum* dihydroorotate dehydrogenase (*Pf*DHODH) inhibitor program [105]. The C-4 SF₅ analogue **59** (Table 5) provided a two- to three-fold potency improvement over the CF₃ analogue **60** as an inhibitor of *Pf*DHODH. It was suggested that the enhanced potency may be due to the increased hydrophobicity of the SF₅ substituent. In addition to increased potency, the SF₅ analogue **59** exhibited good metabolic stability, promising PK parameters *in vivo* and no apparent liabilities. The 3,5-di-F-analog **61** also provided an interesting illustration of the effect of fluorine substitution. This compound compared well with **60** in many respects but showed significantly improved efficacy *in vivo*. These data illustrate again that the SF₅ group can be a suitable substitute for CF₃ with advantage in an optimization effort.

5 Effects of Fluorine on Metabolic Stability

Metabolic stability is a perpetual concern in drug discovery and there are many factors that govern the metabolism of a given compound. Perturbation of properties such as lipophilicity, polarity, sterics, and conformation can often reduce metabolic liabilities. When modifying a compound, changes must be carefully balanced such that the solution to one problem does not introduce another. One strategy to solving a metabolic stability issue is to identify the metabolic “soft spot”, i.e. the site of oxidation, and then block that site with a substituent resistant to metabolism. One way to accomplish this is to replace a labile/susceptible carbon-bound hydrogen with a fluorine atom. This type of substitution infrequently impairs drug-target interactions and is a strategy that has been employed successfully in many contexts [106–110].

One notable example is the discovery of ezetimibe (**63**) (Fig. 24), a marketed β-lactam derivative that lowers systemic cholesterol levels by blocking intestinal absorption of cholesterol [108, 109]. A key experiment led to the identification of active metabolites of the prototype compound **62** after dosing to rats [108], which in turn led to the discovery that metabolites were more efficiently localized to the putative site of action of the drug than **62** itself. Additional studies elucidated the

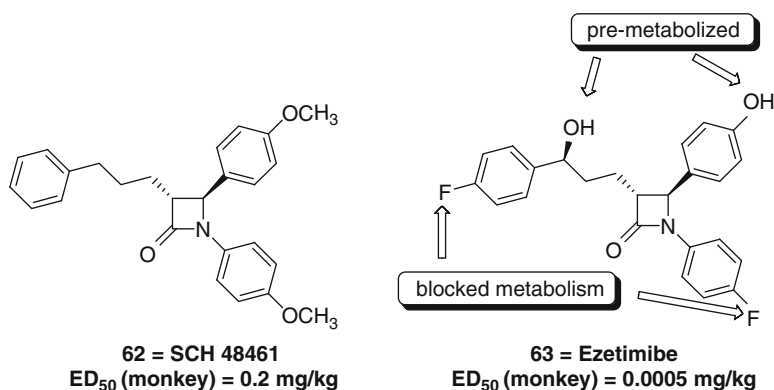


Fig. 24 The structure of ezetimibe (**63**) and its progenitor **62**

structure of several metabolites, some of which offered advantageous localization to the intestine while others did not [111]. Armed with this knowledge, a second generation compound was designed in which sites of detrimental metabolism were blocked via strategic incorporation of substituents. The result was ezetimibe (**63**), a compound which contains hydroxyl functionality crucial to activity and selectivity, as well as fluorine atoms in two key locations which serve to blocked detrimental metabolic pathways without adversely affecting cholesterol absorption inhibitory activity significantly.

The metabolism of heterocycles which leads to reduced potency, poor PK properties or bioactivation into chemically reactive species is a particular concern in drug design, and strategies to mitigate these pathways have been reviewed and summarized [112]. As demonstrated by the discovery of ezetimibe (**63**), if the site of metabolism is known or even presumed, a useful and common strategy is to simply block that position with a fluorine atom. In a thorough effort towards improving metabolic stability in a series of piperidine-based 11β -hydroxysteroid dehydrogenase type I (11β -HSD1) inhibitors, it was discovered that introducing fluorine or polar substituents led to an increase in metabolic stability [113]. It can be reasoned that polar groups lowered the lipophilicity and $\log D$, likely contributing to the increase in metabolic stability. Moreover, in a modification that presumably blocked a metabolic soft spot present in **64** (Fig. 25), installation of a *para*-fluoro substituent (**65**) had a positive effect on metabolic stability in mouse liver microsomes (MLM); a MLM $T_{1/2}$ of >30 min was demonstrated which compared favorably with the unsubstituted piperidine analogue **64**, which exhibited a $T_{1/2}$ of just 6 min.

As suggested above, high lipophilicity can have an adverse impact on metabolic stability. In an effort to improve the metabolic stability of the lead histamine 3 receptor (H_3R) inverse agonist **66** (Fig. 26), ring contraction of the azepine ring coupled with the introduction of fluorine substitution was explored [114]. While there was some confidence that this strategy would lead to increased metabolic

compound	X	MLM $t_{1/2}$ (min)
64		6
65		> 30

Fig. 25 Mouse liver microsome (MLM) half-life data for piperidine-based 11 β -hydroxysteroid dehydrogenase type I (11 β -HSD1) inhibitors

	66	67	68	69
clearance RLM = (μ L/min/mg)	55	17	9	12

Fig. 26 Rat liver microsome (RLM) clearance values for several histamine 3 receptor (H_3R) inverse agonists

stability, there was concern that the structural changes would adversely affect solubility. In the event, the smaller ring size associated with piperidines **67** and **68** resulted in more stable molecules with rat liver microsome (RLM) clearance values of 17 and 9 μ L/min/mg, respectively, as compared to an RLM clearance of 55 μ L/min/mg for **66**. However, the structural changes were accompanied by some adverse affects, with **68** inhibiting the hERG channel by 73 % at a concentration of 10 μ M. Attention was thus shifted toward the morpholine analogue **69** which had reasonable metabolic stability and did not share the hERG liability.

While these examples demonstrate the beneficial effect of blocking metabolism by taking advantage of the inherent strength of a carbon-fluorine bond, in extreme cases this property may be disadvantageous. An example of such a situation was observed in the discovery of SC-58635 (**70**), a cyclooxygenase 2 (COX 2) inhibitor known generically as celecoxib (Fig. 27). The early lead molecule **71** possessed a 4-fluorophenyl moiety that rendered the molecule extremely metabolically stable *in vivo*, represented by the greater than 220 h half life measured in rats [115]. Interestingly, a similar high level of metabolic stability was observed with the chloro analog **72** which had a measured half life of 117 h in rats. In an effort to bring this value into a more acceptable range, the introduction of functionality with greater

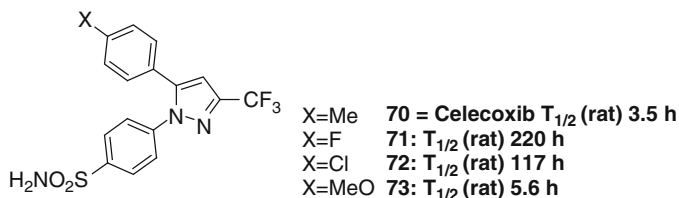


Fig. 27 Rat *in vivo* half life data for celecoxib and related analogues

susceptibility to metabolism was examined. As such, the methoxy analog **73** and the methyl derivative **70** were prepared with both compounds exhibiting a shorter half life in the rat: 5.6 and 3.5 h, respectively.

There are several interesting cases where the introduction of a fluorine atom does not prevent metabolic oxidation at the site of deployment [15]. A specific example is observed in phenyl rings that incorporate a nitrogen substituent *para* to the fluorine atom. In this arrangement, P450-catalyzed oxidation can facilitate fluorine rearrangement to the adjacent carbon atom resulting in a hydroxyl moiety being installed on the carbon atom vacated by the fluorine [116–118].

6 The Effect of Fluorine Substitution on Membrane Permeability

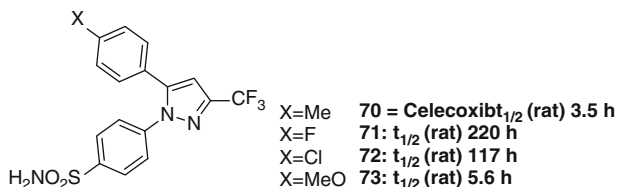
Absorption of an orally administered drug is governed primarily by one of two processes: passive transport, or active transport which requires energy that is typically supplied by ATP. The majority of drugs permeate membranes passively, the ease of which depends on the properties of both the membrane and the diffusing molecule. Membranes are a highly organized, anisotropic system with sufficient fluidity to allow translational and rotational movements of the constituent lipid and protein molecules; the packing density of the constituent elements influences binding to and permeation of drugs [119–121]. Lipophilicity and the cross sectional area of a drug are the two most influential properties governing membrane binding [121]. While the ability of fluorine to influence permeability may diminish with the size of a molecule, it is well suited for use in modulating lipophilicity in the context of small molecule drug discovery.

Lipophilicity is often expressed as $\log P$, the logarithm of the partition coefficient of a compound between octanol and water. A distribution coefficient ($\log D$) is also used to quantify lipophilicity in the event that charge states need to be taken into consideration. A $\log D$ value is the logarithm of the coefficient of the distribution of a molecule between water and octanol at a particular pH, typically 7.4 because of physiological relevance. Based on an analysis of the physical properties of orally bioavailable drugs, the optimal $\log P$ for an orally administered drug is between 1 and 5 [122].

It is a misconception to assume that fluorination of a molecule always increases lipophilicity. Monofluorination or trifluorination of saturated alkyl groups often

Table 6 log *P* (octanol-H₂O) measurements for fluoroalkanes and fluoroalcohols

Fluoroalkane	log <i>P</i>	Fluoroalcohol	log <i>P</i>	Fluoroalcohol	log <i>P</i>
CH ₃ CH ₃	1.81	CH ₃ CH ₂ OH	-0.32	CF ₃ (CH ₂) ₃ OH	0.90
CH ₃ CHF ₂	0.75	CF ₃ CH ₂ OH	0.36	CF ₃ (CF ₂) ₂ CH ₂ OH	1.94
CH ₃ (CH ₂) ₃ CH ₃	3.11	CH ₃ (CH ₂) ₂ OH	0.34	CH ₃ (CH ₂) ₄ OH	1.19
CH ₃ (CH ₂) ₃ CH ₂ F	2.33	CF ₃ (CH ₂) ₂ OH	0.39	CF ₃ (CH ₂) ₄ OH	1.15
		CH ₃ (CH ₂) ₃ OH	0.88		

Fig. 28 *In vivo* efficacy and log *P* of leukotriene receptor antagonists

decreases lipophilicity due to the relatively polar character of the monfluoro- and trifluoro-methyl alkanes which possess highly polar C-F and C-CF₃ bonds. The same is true for difluorination when fluorine is introduced at the terminal carbon atom of an alkane (Table 6) [123]. In contrast to the data shown in Table 6, lipophilicity is typically increased upon aromatic fluorination, perfluorination, and fluorination adjacent to atoms with π -bonds, with the notable exception of some α -fluorinated carbonyl compounds [123]. Presumably, in these cases the lipophilicity is increased due to the excellent overlap between the F-C 2p orbitals which results in significant resonance electron-donation from fluorine to carbon that offsets the inductive electron-withdrawing influence of fluorine.

The situation becomes far less predictable when a heteroatom is proximal to the site of fluorine substitution. As indicated in Table 6, fluorination has little effect on lipophilicity when the site of fluorination is less than 3C-C bonds away, at least in the case in the case of terminal trifluoromethylated alcohols [123].

The impact of fluorine substitution on lipophilicity (as measured by log *P*) has been studied in the context of leukotriene (LT) receptor antagonists [124]. Leukotrienes are signalling molecules responsible for triggering constriction of smooth muscle, and the overproduction of leukotrienes is implicated in contributing to asthma in humans. The development of LT receptor antagonists is one approach towards moderating the bronchoconstrictive properties of leukotrienes. For a series of indole carboxamide-based LT antagonists represented by **74** (Fig. 28), an increase in lipophilicity *via* the careful installation of a trifluoromethyl group led to an increase in efficacy and oral availability. Extending the length of the alkyl chain of the indole amide led to increased lipophilicity but was also associated with a loss in affinity for the LT receptor. Fluorine substitution increased lipophilicity and, in comparison to non-fluorinated analogs, increased *in vivo* potency ten-fold. In a head-to-head comparison, the fluorinated analogs consistently exhibited greater lipophilicity than the non-fluorinated analog as measured by log *P* (Fig. 28).

	R	R'	Caco-2 permeability
75	CH ₃	H	1.20 × 10 ⁻⁶ cm/s
76	CH ₃	F	3.14 × 10 ⁻⁶ cm/s
77	CF ₃	H	3.38 × 10 ⁻⁶ cm/s
78	CF ₃	F	4.86 × 10 ⁻⁶ cm/s

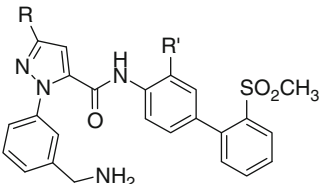


Fig. 29 Caco-2 permeability for a series of pyrazole-based factor Xa inhibitors

	R	R'	IKKβ IC ₅₀	Log <i>D</i>	PAMPA <i>P_e</i>
79	H	H	55 nM	1.8	0.84 × 10 ⁻⁶ cm/s
80	F	H	64 nM	1.8	19 × 10 ⁻⁶ cm/s
81	F	F	27 nM	3.1	> 50 × 10 ⁻⁶ cm/s

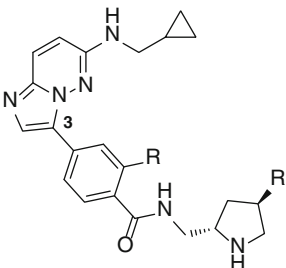


Fig. 30 *In vitro* potency, log *D* and permeability of a series of imidazo[1,2-*b*]pyridazine-based IKKβ inhibitors

The influence of fluorine substitution on permeability, as measured across a Caco-2 bilayer, has been studied in a series of factor Xa (fXa) inhibitors [125, 126]. It was observed during the optimization of the series of pyrazole-based fXa inhibitors **75–78** shown in Fig. 29 that the substitution of the aromatic ring with fluorine afforded a greater than two-fold increase in Caco-2 permeability (**75** vs. **76**). Similarly, the exhaustive introduction of fluoro to the methyl substituent bound to the aromatic ring (CH₃ to CF₃) resulted in a similar improvement in Caco-2 permeability (**77** vs **75**). Further, when both the aromatic ring and the methyl substituent were substituted with fluorine (**78**) the Caco-2 measured permeability increased to 4.86 × 10⁻⁶ cm/s, a >four-fold improvement over that non-fluoro analog **75**. Furthermore, the increased permeability of **78** was complemented by the best *in vivo* potency within the series and **78** also exhibited a high selectivity ratio for fXa versus thrombin (1,000-fold) and fXa versus trypsin (300-fold).

The advantageous impact of fluorine on permeability has been explored in the discovery of a family of imidazo[1,2-*b*]pyridazine-based IKKβ inhibitors where it was assumed that the central benzamide played a key role in pharmacokinetic properties [127]. As shown in Fig. 30, modifications to the benzamide region (C-3) of the imidazo[1,2-*b*]pyridazine had a dramatic affect on permeability: the measured PAMPA values for **79** and **80** were 0.84 × 10⁻⁶ cm/s and 19 × 10⁻⁶ cm/s, respectively [128]. Although **79** and **80** differ by only a single F-for-H substitution, the observed improvement in permeability is presumed to arise from a combination of factors. These factors include the enhancement of hydrophobicity and the formation of a weak interaction between the fluorine atom and the NH moiety, possibly a dipolar interaction.

While the inhibitory activity and $\log D$ of **79** and **80** remained essentially identical, the installation of a second fluorine on the pyrrolidine moiety (**81**) resulted in an increase in both the measured $\log D$ and PAMPA values. In the case of **81**, the added lipophilicity coupled with the small difference in size between H and F also afforded a two-fold increase in potency compared to **79** and **80**.

6.1 Inter- and Intra-molecular H-Bonding of Fluorine

Numerous X-ray crystallographic structures of fluorine-containing compounds demonstrate close inter- and intra-molecular C-F \cdots H contacts and the strong hydrogen-bonding capacity of hydrofluoric acid has long been recognized [30, 129–132]. The intriguing possibility that optimization of C-F \cdots H contacts might lead to an increase in the potency of pharmaceutical agents has, in part, contributed to a significant interest in determining the capacity of fluorine to act as a hydrogen-bond acceptor. Even though the nature of this interaction remains a topic of considerable debate, it is recognized that the C-F \cdots H interaction is much weaker than that of O \cdots H hydrogen-bonding, and that interpretation of possible C-F \cdots H interactions requires care and attention to multiple factors [20, 129, 133–138].

Due to the strong electronegativity of fluorine, the three lone pairs of electrons are tightly held, resulting in fluorine being a poorly polarizable atom [16, 20]. However, the substantial ionic nature of the C-F bond gives rise to a large dipole moment (μ). For example, in fluoromethane the dipole moment is 1.85 D while in difluoromethane it is 1.97 D [20]. In systems such as 3-fluoropiperidinium, dipole minimization rather than C-F \cdots H bonding has been suggested to best explain the observed conformational bias [55]. The C-F \cdots H interaction is variously described as a hydrogen-bonding or a dipolar interaction. The distinction is that a hydrogen-bonding interaction has a covalent component which is anisotropic, while a dipolar interaction is entirely electrostatic and not dependent on directionality. A recent analysis of C-F \cdots H contacts documented in the Cambridge Structural Database (CSD) supports the absence of an anisotropic component in the C-F \cdots H interaction. Specifically, in a survey of 100 compounds with C-F \cdots H bond distances between 1.85 Å and 2.35 Å, the C-F \cdots H bond angle was found to vary significantly between 95° and 165°, while demonstrating no dependence on F \cdots H distance [30]. The absence of a directional dependence of C-F \cdots H interactions is in agreement with an earlier analysis of the Protein Data Bank (PDB) [129]. The C-F \cdots H interaction is therefore best described as a dipolar interaction.

The presence of inter- and intra-molecular C-F \cdots H contacts is mostly supported by crystallographic data. Often a F \cdots H distance shorter than the sum of the F and H van der Waals radii (~ 2.65 Å) is used as evidence for a C-F \cdots H interaction [129]. A review of the PDB in 2004 using this distance criterion as well as directional constraints found that “...there is an 18% chance that a generic PDB entry with a co-crystallized fluorine-containing ligand presents a hydrogen-bond occurring at the fluorine” and that “10% of the overall amount of fluorine atoms from the PDB

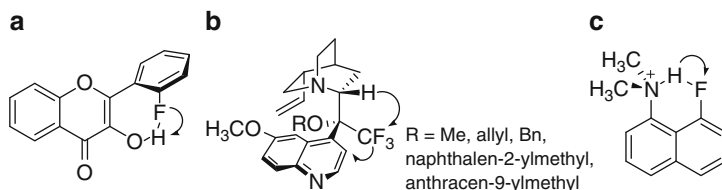


Fig. 31 C-F...H interaction in (a) 2'-fluoroflavonol; (b) O-alkyl 9-dehydro-9-trifluoromethyl-9-epiquinidines; (c) 8-fluoro-*N,N*-dimethylnaphthalen-1-amine

are involved in hydrogen bonding contacts” [129]. The mean F...H distances calculated for aliphatic, aromatic, and geminal fluorines (CF₂H, CF₃) are 2.113 Å, 2.698 Å, and 2.350 Å, respectively. When standard deviation values are considered, the differences between the three types of C-F bond are not statistically significant. Instead, a calculated mean F...H distance of 2.313 Å is more appropriate [129]. As a comparison, almost all H...O and H...N contacts observed crystallographically are less than 2.2 Å in length [138]. It is therefore suggested that a bond distance much shorter than 2.65 Å is often needed for a productive F...H interaction, and that this distance criterion is not a reliable indicator of F...H interactions [137].

Many studies have attempted to provide non-crystallographic evidence for a C-F...H interaction. For example, the magnitude of a ¹*J*_{F,H(O)} NMR coupling constant has been used as evidence for a C-F...H interaction in 2'-fluoroflavonol (Fig. 31a) [139]. However, this analysis targets a minor conformer of 2'-fluoroflavonol and relies upon several assumptions regarding electronics. The same authors report that the ¹*J*_{F,H(O)} coupling constants found for 2-fluorophenol and 4-bromo-2-fluorophenol arise from overlap of the electronic clouds surrounding both coupling nuclei (owing to their spatial proximity) rather than from transmission through a hydrogen bond [140].

In another study, the nature of intramolecular C-F...H-C bonding was interrogated using O-alkyl 9-dehydro-9-trifluoromethyl-9-epiquinidines as model systems (Fig. 31b) [134]. These compounds demonstrate many phenomena consistent with C-F...H-C bonding: X-ray crystal structures contain close F...H contacts, as low as 2.19 Å when R=Me; ¹⁹F NMR spectra contain three distinct resonances with first order ²*J*_{F-F} coupling indicating that the rotation of the CF₃ group is greatly restricted; and noticeable deshielding is observed in ¹H NMR for the proton most proximal to the CF₃ group. A combination of crystallographic and NMR observations with Eyring analysis and extensive computational analysis were used to probe the nature of this C-F...H-C interaction [134]. Despite the strong appearance of a C-F...H-C bonding interaction, it was concluded that steric crowding is responsible for the short F...H distances and restricted rotation; even the strongest C-F...H-C bonding interactions in the system contribute minimally to the ground state geometry or hinder rotation [134].

In contrast to C-F...H-C bonding, the C-F...H-N⁺R₃ interaction is considered one of the strongest C-F...H bonding interactions. As a tool to further study the C-F...H-N⁺R₃ interaction, 8-fluoro-*N,N*-dimethylnaphthalen-1-amine, the fluoro analog of 1,8-bis(dimethylamino)naphthalene (“Proton Sponge”), was prepared and studied (Fig. 31c) [133]. The basicity of this compound is slightly greater (<1 p*K*_a

unit) than that of the parent compound *N,N*-dimethylnaphthalen-1-amine. Crystal structures of the protonated molecule with either a TfO⁻ or B(C₆F₅)₄⁻ counterion indicate an intramolecular C-F...H-N⁺R₃ bonding interaction, with F...H distances of 2.131 Å and 2.027 Å, respectively. In both cases, hydrogen-bonding is observed between the proton and the counterion with significance equal to that of the C-F...H-N⁺R₃ contact. Unlike Proton Sponge, the H-N⁺R₃ proton is observed crystallographically to lie outside of the naphthalene plane, with deviations from planarity of 39.5° and 29.5° for TfO⁻ and B(C₆F₅)₄⁻ counter ions, respectively. Observation in ¹⁹F NMR of a large *J*_{F,H} coupling constant is cited as further support of the C-F...H-N⁺R₃ bonding interaction. Interestingly, the *J*_{F,H} coupling observed with a B(C₆F₅)₄⁻ counterion is suppressed if TfO⁻ or Cl⁻ are instead used as the counterion, or if the solvent for the B(C₆F₅)₄⁻ counterion is switched from CH₂Cl₂ to acetonitrile. Taken together, the evidence points towards the existence of a weak C-F...H-N⁺R₃ interaction which, in terms of significance, is of approximately equal in magnitude to that of the TfO⁻...H interaction.

The large number of C-F...H contacts observed in crystallographic databases may mislead into an overly optimistic assessment of the importance of this interaction. Care must be taken in attributing the interaction to C-F...H bonding rather than to other conformational or intramolecular influences. Where the strongest isolated C-F...H interaction, C-F...H-N⁺R₃, is in fact relatively weak, less significant C-F...H interactions become negligible. However, even weak interactions can play a supporting role in drug-target interactions and, as the prevalence of C-F...H contacts observed crystallographically suggests, the significance of the C-F...H interaction may be amplified in specific environments such as within the cavity of a protein. That the potency of a compound can be increased *via* fluorine substitution is clear, but the contributing factors are likely complex in origin.

7 Fluorine in Positron Emitting Tomography (PET) Imaging

PET imaging has emerged as a useful *in vivo* imaging technique that is non-invasive in nature and is useful in both a pre-clinical and clinical setting. Positrons are antimatter to electrons and encounters between the two particles lead to annihilation and the release of energy in the form of two photons of light. These photons are of high energy (511 keV), travel in opposing directions, and are readily detected simultaneously by PET cameras surrounding the subject [141, 142]. Of particular utility, the coupling of a PET camera with a computed tomography (CT) scanner allows both anatomy and metabolism data to be combined into a unique image [141, 142]. Molecules containing PET atoms are proving to be useful for probing biochemical aspects of disease *in vivo* and drug target engagement [141–146]. The utility of the ¹⁸F isotope in PET imaging relies upon its 110 min decay half life, the longest of all of the short-lived positron-emitting radionuclides with applicability in small molecule imaging (Table 7), and the facility with which drug molecules will accommodate fluorine as a substitute for a hydrogen atom whilst preserving fundamental

Table 7 Half lives for decay and products of the most commonly used radionuclides in PET imaging

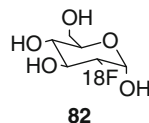
Radionuclide	T _{1/2} (min)	Product
¹¹ C	20.4	¹¹ B
¹³ N	9.97	¹³ C
¹⁵ O	2.04	¹⁵ N
¹⁸ F	110	¹⁸ O

biological properties [141–146]. However, this aspect of biochemistry must be determined by careful experimentation, particularly in the context of allosteric modulators where structure-activity relationships can be subtle and small structural changes can invert pharmacological properties [147–150]. In addition, the energy of the positron emitted by ¹⁸F is such that it travels only short distances before the annihilation event, effectively localizing the signal within a specific tissue. The utility of ¹⁸F in PET imaging is further amplified by the frequency with which fluorine atoms are being incorporated into contemporary drug candidates and marketed drugs as medicinal chemists seek to take advantage of the unique and sometimes enigmatic properties that can be conferred by this atom [15–19, 67]. Recent estimates suggest that 20 % of the drugs in the current pharmacopeia and 9 of the 30 best selling small molecule drugs (*vide supra*) in 2009 contain fluorine, providing an opportunity to introduce the ¹⁸F isotope in a fashion that would be expected to exert no demonstrable effect on the biological profile of a prototype molecule [17, 67].

Against this backdrop, ¹⁸F derivatives have emerged as important tools in biomedical imaging, with broad application essentially limited only by the methodology to introduce this isotope into molecules in a convenient fashion at the very last stages of compound synthesis and under mild conditions that preserve molecular integrity [151–158]. Production of ¹⁸F requires a cyclotron in which, most commonly, ¹⁸O-enriched water is bombarded with accelerated protons to produce [¹⁸F] fluoride ions ([¹⁸F]F⁻) which are trapped on an ion exchange resin for the purpose of separation and released by using a carbonate or bicarbonate solution containing the appropriate metal counter ion. However, fluoride ion is poorly nucleophilic but quite basic, a problem solved by elution with a solution of 2,2,2-cryptand and K₂CO₃ in CH₃CN which, after drying, provides a complex of [(crypt-222)K]⁺[¹⁸F]⁻ in which chelation of the potassium ion increases fluoride reactivity [141]. The highly electrophilic [¹⁸F]-fluorine gas ([¹⁸F]F₂) can also be prepared in a cyclotron by bombarding natural neon with high energy deuterons or, preferably, ¹⁸O₂ with protons to provide alternative reactivity pathways with which to introduce ¹⁸F.

2-[¹⁸F]-Fluoro-2-deoxy-D-glucose ([¹⁸F]-FDG, **82**) has found widespread application for assessing the metabolic status of heart, lungs and brain and, particularly, for imaging tumor cells, which accumulate the molecule based on their high metabolic demands (Fig. 32) [159]. [¹⁸F]-FDG (**82**) is recognized as glucose and taken up by cells *via* the glucose transporter and phosphorylated by hexokinase to [¹⁸F]-FDG-6-phosphate, which cannot be metabolized further due to the presence of the 2-fluorine substituent [142, 143]. This maximizes the value of [¹⁸F]-FDG (**82**) as a PET agent by localizing the molecule and preventing its metabolic conversion into a myriad of degradation products. Moreover, decomposition of [¹⁸F]-FDG (**82**)

Fig. 32 2- ^{18}F -Fluoro-2-deoxy-D-glucose (^{18}F -FDG)



ultimately affords 2- ^{18}O glucose, a heavy atom analogue that is innocuously metabolized by normal pathways. ^{18}F -FDG (**82**) is used to diagnose a range of cancers including lung and intestinal cancer, lymphomas and melanomas and metastatic tumors but is not without its limitations as a diagnostic tool since its utility is dependent on tumor location and homogeneity [142].

The radiolabeling of ligands for specific receptors, transporters or enzymes with ^{18}F provides reagents of particular value for the development and assessment of central nervous system (CNS) function *in vivo* in a non-invasive fashion that has both preclinical and clinical utility [142]. In addition to providing insights into brain metabolism and neurotransmission, ^{18}F -labeled ligands can be used to provide evidence of brain distribution and target engagement by an exploratory drug candidate for which a homologue incorporating a positron emitting element has been identified. However, the development of PET ligands to label specific receptors in the brain is not always straightforward and success depends on several factors including the intrinsic affinity of a ligand for the protein target of interest, specific radioactivity of the probe molecule, susceptibility to metabolic degradation that leads to loss of the radiolabel, blood-brain barrier permeability of the compound which can be a function of P-glycoprotein-mediated efflux, and the extent of non-specific binding to tissues which can lead to poor signal contrast [143, 144]. The latter is often a function of molecules that are highly lipophilic and which are attracted with facility to fatty acid elements in cell membranes, providing high background signals that are manifested as noise. For optimal brain penetration, a $\log P$ value of between 1.5 and 3 is generally considered to be optimal although $\log D$ measurements that take into account the charge at the physiological pH of 7.4 are considered to be the more relevant index of lipophilicity [143]. However, there are exceptions to these guidelines and the development of ^{18}F -labeled PET ligands remains an experimental science.

Many useful PET ligands that demonstrate specificity for target receptors, transporters or enzymes have been developed, and these ligands have proven useful as probes for imaging receptor occupancy, monitoring changes in target density, and measuring *in vivo* drug distribution and kinetics after local administration, particularly to the CNS and the lung (Fig. 33) [144, 160–163]. A prominent example is ^{18}F -fluoro-L-DOPA (**83**), the first agent developed to image the dopamine system. **83** is used as a metabolic tracer to characterize neuroendocrine tumors which take up ^{18}F -FDG (**82**) only poorly and to monitor dopamine distribution and metabolism in the brain where it is converted to ^{18}F -fluorodopamine (**84**) and additional metabolites useful in the study of Parkinson's disease [144, 164–167]. ^{18}F -2- β -carbomethoxy-3- β -(4-chlorophenyl)-8-(2-fluoroethyl)-nortropane (^{18}F -FECNT) (**85**) is an analogue of cocaine used to assess the density of presynaptic dopamine transporters whilst ^{18}F -fallypride (**86**) is a useful ligand for labeling the dopamine D2 receptor [144, 168–170].

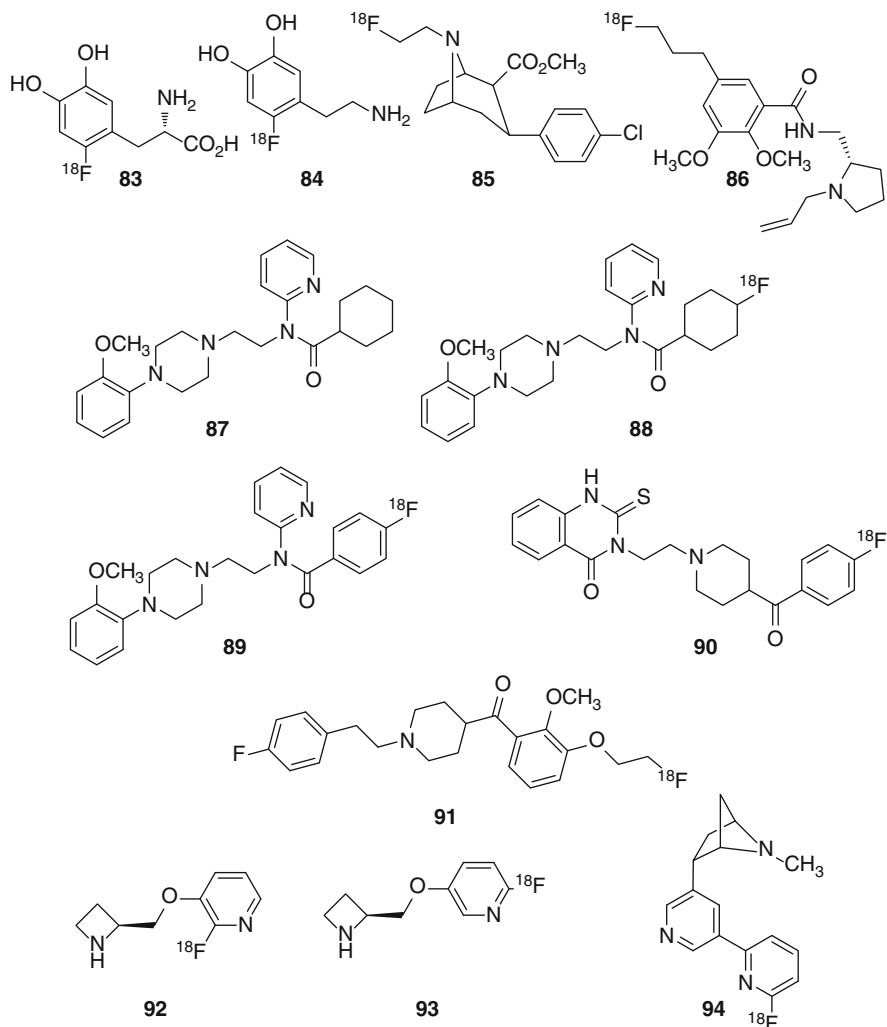


Fig. 33 PET ligands that have been used to target receptors, transporters or enzymes

WAY-100635 (**87**) was originally described as a potent and selective 5HT_{1A} receptor antagonist, $K_i=2.2$ nM, prompting the development of labeled forms used to illuminate the pharmacology of these receptors *in vivo* [144, 171]. A ^{11}C label was readily introduced at the carbonyl carbon for PET imaging since the absence of fluorine in the molecule prevented simple replacement, necessitating the development and profiling of the analogues **88** and **89** in order to take advantage of the properties of ^{18}F [172]. However, more recent studies have revealed that **87** binds to dopamine $D_{4.2}$ receptors with a $K_i=16.4$ nM where it acts as a full agonist, providing caution on the use of **87** and its analogues in imaging [171].

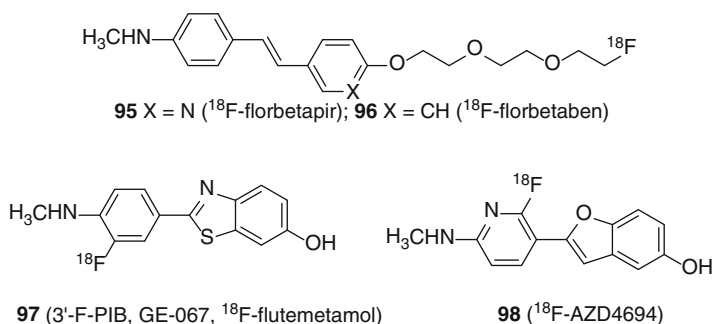


Fig. 34 PET tracers for the detection of A β amyloid plaques

^{18}F -Altanserin (**90**) is used to label 5HT $_2\text{A}$ receptors while MA-1 (**91**) offers enhanced receptor selectivity and lipophilicity [144, 173, 174]. 2-[^{18}F]-F-A85380 (**92**) and 6-[^{18}F]-F-A85380 (**93**) have been developed as useful PET ligands for labeling the nicotinic acetylcholine receptor but take several hours to reach steady state concentration in the brain and exhibit low binding potentials ($B_{\text{max}}/K_{\text{d}}$), prompting the development of **94** as a $\alpha 2\beta 4$ antagonist, $K_{\text{i}} = 240$ pM, with improved brain kinetics [144, 175].

The ^{18}F -labelled styrylpyridine derivative florbetapir (**95**) was approved by the FDA on April 6th, 2012 for use as a PET ligand that labels A β amyloid plaques in the brain (Fig. 34) [176, 177]. ^{18}F -Florbetapir (**95**) derives from a series of stilbene derivatives that labeled amyloid plaques but were too lipophilic to be practically useful since they afforded high levels of non-specific binding in healthy brain [178–187]. The replacement of one of the phenyl rings with a pyridine heterocycle coupled with the introduction of a short polyethylene glycol moiety terminating with fluorine substitution provided **95**, a molecule with improved physical properties that bound to amyloid A β aggregates from post-mortem Alzheimer's disease brain tissue with a K_{d} of 3.72 nM and a B_{max} of 8,811 fmol/mg protein [185]. Licensing of ^{18}F -florbetapir (**95**) was based on the results of a Phase 3 clinical trial conducted in 29 patients dying of Alzheimer's disease in which the amyloid A β plaque levels estimated by the tracer were compared with post-mortem samples, an analysis that revealed excellent concordance [187]. Three additional amyloid plaque labeling agents in clinical trials are ^{18}F -florbetaben (**96**), a close analogue of ^{18}F -florbetapir (**95**), ^{18}F -flutemetamol (**97**) and ^{18}F -AZD4694 (**98**) [188–196].

The introduction of ^{18}F into potential PET ligands requires synthetic methodology that allows late stage installation of the radiolabel under conditions that are compatible with inherent and potentially labile functionality [141–145, 197]. The most common method of introducing ^{18}F into an alkyl chain relies upon ^{18}F fluoride displacement of a leaving group, typically a sulfonate, with cryptands used to sequester the counter ion and enhance the reactivity of the weakly nucleophilic anion [141–145, 197]. However, preparative procedures for a number of prosthetic moieties that incorporate alkyl fluorides have been developed that offer some advantage should this element be a part of the candidate molecule [144]. The application

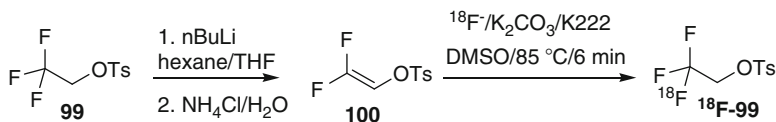


Fig. 35 Preparation of a ^{18}F -fluoroethyl reagent

of microwave heating techniques has markedly facilitated some of these procedures, improving both yields and speed of synthesis. The ^{18}F -fluoroethyl moiety is quite prominent in ^{18}F PET ligands, with the label readily introduced by treating the corresponding tosylate or trifluoromethyl sulfonate derivative with ^{18}F -fluoride [141–145, 168, 169, 197]. ^{18}F -Labeled 2,2,2-trifluoroethyl 4-methylbenzenesulfonate (^{18}F -**99**) is a prosthetic group that offers a useful approach to prepare potential PET ligands and is accessible from the unlabeled material which is sequentially subjected to $n\text{BuLi}$ -mediated elimination of HF to afford the divinyl fluoride **100** which adds ^{18}F quickly and efficiently under mild and carefully optimized conditions (Fig. 35) [198]. ^{18}F -**99** was prepared with good specific radioactivity and readily alkylated 4-cyanophenol, diphenylmethanethiol, 4-chlorobenzoic acid and dibenzylamine rapidly under mild conditions mediated by Cs_2CO_3 as the base in DMF as solvent [198].

Aryl fluorides are a much more common structural motif, ubiquitously explored in lead optimization campaigns where a phenyl ring is part of the pharmacophore. Whilst these moieties offer the potential to prepare an ^{18}F -labeled analogue of a highly optimized ligand, the introduction of fluorine to these rings late in a synthetic scheme can present a considerable challenge and both nucleophilic and electrophilic processes have been developed [141–145, 197].

Aryl or heteroaryl ring fluorination can be accomplished using $^{18}\text{F}^-$ to displace a range of leaving groups, including F, Cl, Br, and I in addition to NO_2 , NMe_3^+ and ArI^+ , a reaction facilitated by the presence of an electron withdrawing moiety on the ring [151–158, 197, 199]. Electrophilic aromatic fluorination processes are more difficult and have typically relied upon the use of $^{18}\text{F}_2$ gas, which is highly reactive and must be used under controlled conditions, with regiochemistry influenced by using trialkyl tin or mercury substituents to direct incorporation [197]. A promising new approach to electrophilic fluorination that exhibits greater compatibility with the kind of functionality found in drug molecules takes advantage of palladium catalysis with the palladium fluoride complex **102** prepared efficiently from **101** by exposure to fluoride for 5 min (Fig. 36) [200]. The palladium fluoride complex **102** functions as an electrophilic fluorinating agent and reacts with Pd-aryl complexes to afford aryl fluorides in good yield when heated in acetone at $85\text{ }^\circ\text{C}$ for 10 min [200]. In a representative example, Pd complex **105** afforded the aryl fluoride **106** in 72 % yield under these conditions. Practical considerations relating this chemistry to ^{18}F labeling applications include the stability of the Pd complexes **101** and **102**, with the former stable at room temperature and to brief air exposure, whilst the palladium fluoride complex **102** is stable at $100\text{ }^\circ\text{C}$ for 24 h and in 10 % aqueous CH_3CN for

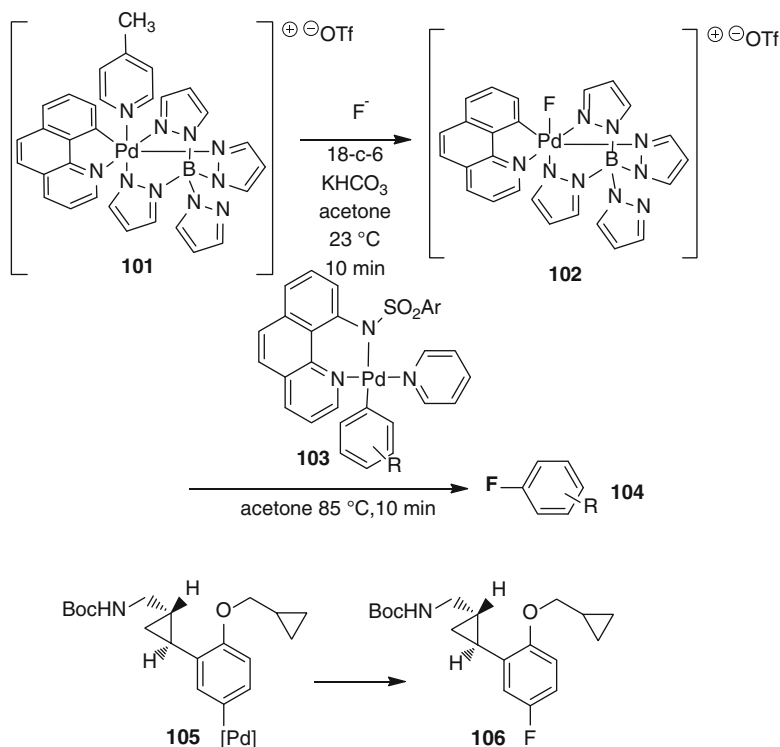


Fig. 36 ^{18}F -Pd complex **102** serves as a useful source of electrophilic ^{18}F

3 h at 23 °C. However, stoichiometric quantities of the catalyst **102** are required and care must be taken to purify the organic products to remove residual Pd. Complex **101** was shown to react with solutions of ^{18}F -prepared under conventional conditions to afford ^{18}F -labelled **102** which provided ^{18}F -labelled **106** in an average 18 % radiochemical yield in two steps from $^{18}\text{F}^-$ [200].

A particularly interesting fluorination process that relies upon fluoride ion as the source and is radical-based in nature takes advantage of the manganese porphyrin catalyst $\text{Mn}(\text{TMP})\text{Cl}$ (**107**) to promote an oxidative fluorination that is applicable to aliphatic C-H moieties, potentially offering wide substrate versatility (Fig. 37) [201]. The experimental protocol exposes substrate to three equivalents of AgF , 6–8 equivalents of iodosylbenzene, 0.3 equivalents of tetrabutylammonium fluoride trihydrate and 6–8 mole % of catalyst **107** in mixture of CH_3CN and CH_2Cl_2 at 50 °C under an inert atmosphere. The active catalyst in this process is believed to be *trans*-difluoro $\text{Mn}^{\text{IV}}(\text{TMP})$ (**108**) which transfers a fluorine atom to a carbon radical generated by a Mn^{V} oxo species produced by iodosylbenzene oxidation, as depicted in the catalytic cycle shown in Fig. 37. The procedure provides products in modest yields, typically just below 50 %, and with generally poor stereoselectivity at sites that are electronically unactivated. Nevertheless, the procedure is compatible

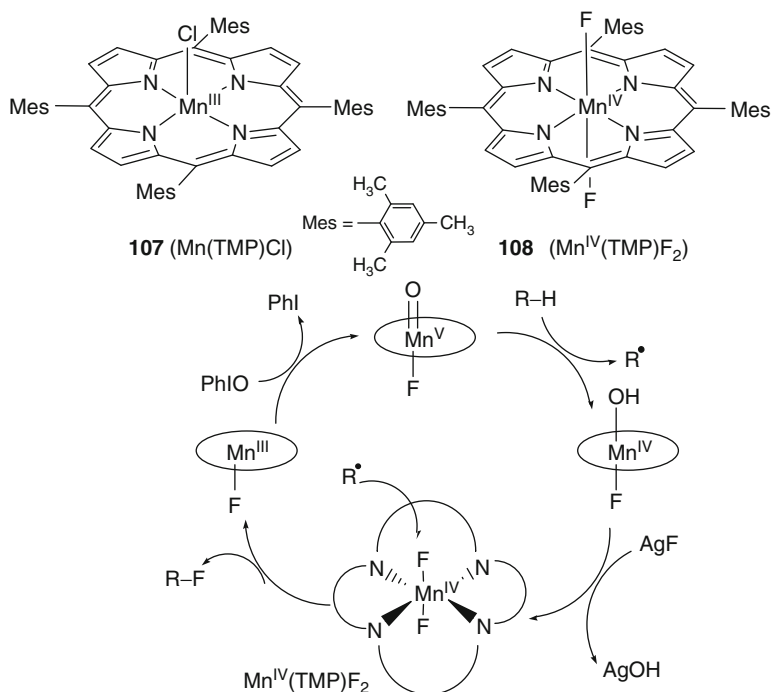


Fig. 37 Catalytic cycle for the fluorination of aliphatic substrates initiated by the manganese porphyrin derivative **107**

with a wide range of functional groups and provides access to compounds that would otherwise require significant synthetic manipulation to access by a *de novo* approach.

8 Conclusion

Fluorine is a unique atom that has found widespread application in drug design to address problems associated with controlling conformation, enhancing potency, interfering with metabolism, increasing membrane permeability and modulating the pK_a of proximal functionality. Although the physical chemistry underlying many of these effects is reasonably well understood, there remains much to learn about the influence of fluorine on drug properties and how fluorine can be exploited to full advantage. With continuing advances in the development of mild and efficient methods to introduce fluorine into organic molecules, it can be anticipated that applications of this remarkable element in drug discovery and development will grow in both sophistication and understanding. The promise of new and deeper insights into the properties and utility of fluorine should provide additional creative stimulus for improved synthetic methods, broadening and enhancing productive applications.

References

1. Vulpetti A, Hommel U, Landrum G, Lewis R, Dalvit C (2009) Design and NMR-based screening of LEF, a library of chemical fragments with different local environments of fluorine. *J Am Chem Soc* 131:12949–12959
2. Jordan JB, Poppe L, Xia X, Cheng AC, Sun Y, Michelsen K, Eastwood H, Schnier PD, Nixey T, Zhong W (2012) Fragment based drug discovery: practical implementation based on ^{19}F NMR spectroscopy. *J Med Chem* 55:678–687
3. Vulpetti A, Dalvit C (2012) Fluorine local environments: from screening to drug design. *Drug Discov Today* 17:890–897
4. Harper DB, O'Hagan D, Murphy CD (2003) The handbook of environmental chemistry, vol 3 Part P. Springer, Berlin/Heidelberg, pp 141–169
5. Bowen HJM (1966) Trace elements in biochemistry. Academic, London
6. Sharpe AG (1967) In: Gutmann V (ed) Halogen chemistry, vol 1. Academic, New York, p 12
7. Neidleman SL, Geigert J (1986) Biohalogenation: principles, basic roles and applications. Ellis Horwood Ltd, Chichester
8. Vaillancourt F, Yeh E, Vosburg DA, Garneau-Tsodikova S, Walsh CT (2006) Nature's inventory of halogen catalysts: oxidative strategies predominate. *Chem Rev* 106:3364–3378
9. O'Hagan D (2006) Recent developments on the fluorinase of *Streptomyces cattleya*. *J Fluor Chem* 127:1479–1483
10. Zhu X, Robinson DA, McEwan AR, O'Hagan D, Naismith JH (2007) Mechanism of enzymatic fluorination in *Streptomyces cattleya*. *J Am Chem Soc* 139:14597–14604
11. Wagner C, El Omari M, König GM (2009) Biohalogenation: nature's way to synthesize halogenated metabolites. *J Nat Prod* 72:540–553
12. Meyer M, O'Hagan D (1992) Rare fluorinated natural products. *Chem Br* 28:785
13. Heidelberger C, Chaudhuri NK, Danneberg P, Mooren D, Griesbach L, Duschinsky R, Schnitzer RJ, Plevin E, Scheiner J (1957) Fluorinated pyrimidines, a new class of tumour-inhibitory compounds. *Nature* 179:663–666
14. Bégué J-P, Bonnet-Delpon D (2008) Bioorganic and medicinal chemistry of fluorine. Wiley, Hoboken
15. Böhm H-J, Banner D, Bendels S, Kansy M, Kuhn B, Müller K, Obst-Sander U, Stahl M (2004) Fluorine in medicinal chemistry. *ChemBioChem* 5:637–643
16. Müller K, Faeh C, Diederich F (2007) Fluorine in pharmaceuticals: looking beyond intuition. *Science* 317:1881–1886
17. Hagmann WK (2008) The many roles for fluorine in medicinal chemistry. *J Med Chem* 51:4359–4369
18. Purser S, Moore PR, Swallow S, Gouverneur V (2008) Fluorine in medicinal chemistry. *Chem Soc Rev* 37:320–330
19. Shah P, Westwell AD (2007) The role of fluorine in medicinal chemistry. *J Enzym Inhib Med Chem* 22:527–540
20. O'Hagan D (2008) Understanding organofluorine chemistry: an introduction to the C-F bond. *Chem Soc Rev* 37:308–319
21. Hunter L (2010) The C-F bond as a conformational tool in organic and biological chemistry. *Belistein J Org Chem* 6. doi:103762/bjoc.6.38
22. Zimmer LE, Sparr C, Gilmour R (2011) Fluorine conformational effects in organocatalysis: an emerging strategy for molecular design. *Angew Chem Int Ed* 50:11860–11871
23. Buissonneaud DY, van Mourik T, O'Hagan D (2010) A DFT study on the origin of the fluorine gauche effect in substituted fluoroethanes. *Tetrahedron* 66:2196–2202
24. O'Hagan D (2012) Organofluorine chemistry: synthesis and conformation of vicinal fluoromethylene motifs. *J Org Chem* 77:3689–3699
25. Wu D, Tian A, Sun H (1998) Conformational properties of 1,3-difluoropropane. *J Chem Phys A* 102:9901–9905

26. Tavasli M, O'Hagan D, Pearson C, Petty MC (2002) The fluorine *gauche* effect. Langmuir isotherms report the relative conformational stability of (\pm)-*erythro*- and (\pm)-*threo*-9,10-difluorostearic acids. Chem Commun 1226–1227
27. Hunter L, Kirsch P, Slawin AMZ, O'Hagan D (2009) Synthesis and structure of stereoisomeric multivincin hexafluoroalkanes. Angew Chem Int Ed 48:5457–5460
28. Banks JW, Batsanov AS, Howard JAK, O'Hagan D, Rzepa H, Martin-Santamaria S (1999) The preferred conformation of α -fluoroamides. J Chem Soc Perkin 2:2409–2411
29. Briggs CRS, O'Hagan D, Howard JAK, Yulfi DS (2003) The C-F bond as a tool in the conformational control of amides. J Fluor Chem 119:9–13
30. Dalvit D, Vulpetti A (2012) Intermolecular and intramolecular hydrogen bonds involving fluorine atoms: implications for recognition, selectivity, and chemical properties. ChemMedChem 7:262–272
31. Schöler M, O'Hagan D, Slawin AMZ (2005) The vicinal F-C-C-F moiety as a tool for influencing peptide conformation. Chem Commun 4324–4326
32. O'Hagan D, Rzepa HS, Schöler M, Slawin AMZ (2006) The vicinal difluoro motif: the synthesis and conformation of *erythro*- and *threo*-diastereomers of 1,2-difluorodiphenylethanes, 2,3-difluorosuccinic acids and their derivatives. Beilstein J Org Chem. doi:10.1186/1860-5397-2-19
33. Winkler M, Moraux T, Khaairy HA, Scott RH, Slawin AMZ, O'Hagan D (2009) Synthesis and vanilloid receptor (TRPV1) activity of the enantiomers of α -fluorinated capsaicin. ChemBioChem 10:823–828
34. Peddie V, Butcher RJ, Robinson WT, Wilce MCJ, Traore DAK, Abell AD (2012) Synthesis and conformation of fluorinated β -peptidic compounds. Chem Eur J 18:6655–6662
35. O'Hagan D, Bilton C, Howard JAK, Knight L, Tozer DJ (2001) The preferred conformation of N- β -fluoroethylamides: observation of the fluorine amide *gauche* effect. J Chem Soc Perkin Trans 2:605–607
36. O'Hagan D, Rzepa HS (1997) Some influences of fluorine in bioorganic chemistry. Chem Commun 645–652
37. Holmgren SK, Taylor KM, Bretscher LE, Raines RT (1998) Code for collagen's stability deciphered. Nature 392:666–667
38. Bretscher LE, Jenkins CL, Taylor KM, DeRider ML, Raines RT (2001) Conformational stability of collagen relies on a stereoelectronic effect. J Am Chem Soc 123:777–778
39. Hodges JA, Raines RT (2003) Stereoelectronic effects on collagen stability: the dichotomy of 4-fluoroproline diastereomers. J Am Chem Soc 125:9262–9263
40. Doi M, Nishi Y, Uchiyama S, Nisiuchi Y, Nakazawa T, Ohkubo T, Kobayashi Y (2003) Characterization of collagen model peptides containing 4-fluoroproline: (4(S)-fluoroproline-Pro-Gly)₁₀ forms a triple helix, but (4(R)-fluoroproline-Pro-Gly)₁₀ does not. J Am Chem Soc 125:9922–9923
41. Hodges JA, Raines RT (2005) Stereoelectronic and steric effects in the collagen triple helix: toward a code for strand association. J Am Chem Soc 127:15923–15932
42. Shoulders MD, Kamer KJ, Raines RT (2009) Origin of the stability conferred upon collagen by fluorination. Bioorg Med Chem Lett 19:3859–3862
43. Doi M, Nishi Y, Kiritoshi N, Iwata T, Nago M, Nakano H, Uchiyama S, Nakazawa T, Wakamiya T, Kbayashi Y (2002) Simple and efficient syntheses of Boc- and Fmoc-protected 4(R)- and 4(S)-fluoroproline solely from 4(R)-hydroxyproline. Tetrahedron 58:8453–8459
44. DeRider ML, Wilkins SJ, Waddell MJ, Bretscher LE, Weinhold F, Raines RT, Markley JL (2002) Collagen stability: insights from NMR spectroscopic and hybrid density functional computational investigations of the effect of electronegative substituents on prolyl ring conformations. J Am Chem Soc 124:2497–2505
45. Park S, Radmer RJ, Klein TE, Pande VS (2005) A new set of molecular mechanics parameters for hydroxyproline and its use in molecular dynamics simulations of collagen-like peptides. J Comput Chem 26:1612–1616

46. Hodges JA, Raines RT (2006) Energetics of an $n \rightarrow \pi^*$ interaction that impacts protein structure. *Org Lett* 8:4695–4697
47. Hinderaker MP, Raines RT (2003) An electronic effect on protein structure. *Protein Sci* 12:1188–1194
48. Raines RT (2006) 2005 Emil Thomas Kaiser Award. *Protein Sci* 15:1219–1225
49. Improta R, Mele F, Crescenzi O, Benzi C, Barone V (2002) Understanding the role of stereoelectronic effects in determining collagen stability: a quantum mechanical/molecular mechanical study of (proline-proline-glycine)_n polypeptides. *J Am Chem Soc* 124:7857–7865
50. Kim W, Hardcastle KL, Conticello VP (2006) Fluoroproline flip-flop: regiochemical reversal of a stereoelectronic effect on peptide and protein structures. *Angew Chem Int Ed* 45:8141–8814
51. Kitamoto T, Ozawa T, Abe M, Marubayashi S, Yamazaki T (2008) Incorporation of fluoroprolines to proctolin: study on the effect of a fluorine atom towards peptidic conformation. *J Fluor Chem* 129:286–293
52. Briggs CRS, Allen MJ, O'Hagan D, Tozer DJ, Slawin AMZ, Goeta AE, Howard JAK (2004) The observation of a large *gauche* preference when 2-fluoroethylamine and 2-fluoroethanol become protonated. *Org Biomol Chem* 2:732–740
53. Lankin DC, Chandrakumar NS, Rao SN, Spangler DP, Snyder JP (1993) Protonated 3-fluoropiperidines: an unusual fluoro directing effect and a test for quantitative theories of solvation. *J Am Chem Soc* 115:3356–3357
54. Snyder JP, Chandrakumar NS, Sato H, Lankin DC (2000) The unexpected diaxial orientation of cis-3,5-difluoropiperidine in water: a potent CF – NH charge-dipole effect. *J Am Chem Soc* 122:544–545
55. Sun A, Lankin DC, Hardcastle K, Snyder JP (2005) 3-Fluoropiperidines and N-methyl-3-fluoropiperidinium salts: the persistence of axial fluorine. *Chem Eur J* 11:1579–1591
56. Gerig JT, McLeod RS (1973) Conformation of *cis*- and *trans*-4-fluoro-L-proline in aqueous solution. *J Am Chem Soc* 95:5725–5729
57. Deniau G, Slawin AMZ, Lebl T, Chorki F, Issberner JP, van Mourik T, Heygate JM, Lambert JJ, Etherington L-A, Sillar KT, O'Hagan D (2007) Synthesis, conformation and biological evaluation of the enantiomers of 3-fluoro- γ -aminobutyric acid ((*R*)- and (*S*)-3F-GABA): an analogue of the neurotransmitter GABA. *ChemBioChem* 8:2265–2274
58. Clift MD, Ji H, Deniau GP, O'Hagan D, Silverman RB (2007) Enantiomers of 4-amino-3-fluorobutanoic acid as substrates for γ -aminobutyric acid aminotransferase: conformational probes for GABA binding. *Biochemistry* 46:13819–13828
59. Yamamoto I, Deniau GP, Gavande N, Chebib M, Johnston GAR, O'Hagan D (2011) Agonist responses of (*R*)- and (*S*)-3-fluoro- γ -aminobutyric acids suggest an enantiomeric fold for GABA binding to GABAC receptors. *Chem Commun* 47:7956–7958
60. Chia PW, Livesey MR, Slawin AMZ, van Mourik T, Wyllie DJA, O'Hagan D (2012) 3-Fluoro-N-methyl-D-aspartic acid (3F-NMDA) stereoisomers as conformational probes for exploring agonist binding at NMDA receptors. *Chem Eur J* 18:8813–8819
61. Gooseman NEJ, O'Hagan D, Slawin AMZ, Teale AM, Tozer DJ, Young RJ (2006) The intramolecular β -fluorine \cdots ammonium interaction in 4- and 8-membered rings. *Chem Commun* 3190–3192
62. Campbell NH, Smith DL, Reszka AP, Neidle S, O'hagan D (2011) Fluorine in medicinal chemistry: β -fluorination of peripheral pyrrolidine attached to acridine ligands affects their interactions with G-quadruplex DNA. *Org Biomol Chem* 9:1328–1331
63. Abraham RJ, Chambers EJ, Thomas AW (1994) Conformational analysis. Part 22. An NMR and theoretical investigation of the *gauche* effect in fluoroethanols. *J Chem Soc Perkin Trans* 2:949–955
64. Abraham RJ, Smith TAD, Thomas AW (1996) Conformational analysis. Part 28. OH-F hydrogen bonding and the conformation of *trans*-2-fluorocyclohexanol. *J Chem Soc Perkin Trans* 2:1949–1955

65. Fried J, Sabo EF (1954) 9 α -Fluoro derivatives of cortisone and hydrocortisone. *J Am Chem Soc* 76:1455–1456
66. Fried J (1955) Biological effects of 9 α -fluorohydrocortisone and related halogenated steroids in animals. *Ann N Y Acad Sci* 61:573–581
67. O'Hagan D (2010) Fluorine in health care: organofluorine-containing blockbuster drugs. *J Fluor Chem* 131:1071–1081
68. Mock W, Zhang JZ (1990) Concerning the relative acidities of simple alcohols. *Tetrahedron Lett* 31:5687–5688
69. Weeks CM, Duax WL, Wolff ME (1973) A comparison of the structure of six corticosteroids. *J Am Chem Soc* 95:2865–2868
70. Wolff ME, Baxter JD, Kollman PA, Lee DL, Kuntz ID, Bloom E, Matulich DT, Morris J (1978) Nature of steroid-glucocorticoid receptor interactions: thermodynamic analysis of the binding reaction. *Biochemistry* 17:3201–3208
71. Myers AG, Barbay JK, Zhong B (2001) Asymmetric synthesis of chiral organofluorine compounds: use of nonracemic fluoriodoacetic acid as a practical electrophile and its application to the synthesis of monofluoro hydroxyethylene dipeptide isosteres within a novel series of HIV protease inhibitors. *J Am Chem Soc* 123:7207–7219
72. Leroux F, Jeschke P, Schlosser M (2005) α -Fluorinated ethers, thioethers, and amines: anomerically biased species. *Chem Rev* 105:827–856
73. Massa MA, Spangler DP, Durley RC, Hickory BS, Connolly DT, Witherbee BJ, Smith ME, Sikorski JA (2001) Novel heteroaryl replacements of aromatic 3-tetrafluoroethoxy substituents in trifluoro-3-(tertiaryamino)-2-propanols as potent inhibitors of cholesterol ester transfer protein. *Bioorg Med Chem Lett* 11:1625–1628
74. Horne DB, Bartberger MD, Kaller MR, Monenschein H, Zhong W, Hitchcock SA (2009) Synthesis and conformational analysis of α , α -difluoroalkyl heteroaryl ethers. *Tetrahedron Lett* 50:5452–5455
75. Hehre WJ, Radom L, Pople JA (1972) Molecular orbital theory of the electronic structure of organic compounds. XII. Conformations, stabilities, and charge distributions in monosubstituted benzenes. *J Am Chem Soc* 94:1496–1504
76. Anderson GM III, Kollman PA, Domelsmith LN, Houk KN (1979) Methoxy group nonplanarity in *o*-dimethoxybenzenes. Simple predictive models for conformations and rotational barriers in alkoxyaromatics. *J Am Chem Soc* 101:2344–2352
77. Hummel W, Huml K, Bürgi H-B (1988) Conformational flexibility of the methoxyphenyl group studies by statistical analysis of crystal structure data. *Helv Chim Acta* 71:1291–1302
78. Brameld KA, Kuhn B, Reuter DC, Stahl M (2008) Small molecule conformational preferences derived from crystal structure data. A medicinal chemistry focused analysis. *J Chem Inf Model* 48:1–24
79. Johnson F (1968) Allylic strain in six-membered rings. *Chem Rev* 68:375–413
80. Klocker J, Karpfen A, Wolschann P (2003) On the structure and torsional potential of trifluoromethoxybenzene: an *ab initio* and density functional study. *Chem Phys Lett* 367:566–575
81. Graton J, Wang Z, Brossard A-M, Monteiro DG, Questel J-YL, Linclau B (2012) An unexpected and significantly lower hydrogen-bond-donating capacity of fluorohydrins compared to nonfluorinated alcohols. *Angew Chem Int Ed* 51:6176–6180
82. Meanwell N (2011) Improving drug candidates by design: a focus on physicochemical properties as a means of improving compound disposition and safety. *Chem Res Toxicol* 24:1420–1456
83. Peters JE, Schnider P, Mattei P, Kansy M (2009) Pharmacological promiscuity: dependence on compound properties and target specificity in a set of recent Roche compounds. *ChemMedChem* 4:680–686
84. Azzaoui K, Hamon J, Faller B, Whitebread S, Jacoby E, Bender A, Jenkins JL, Urban L (2007) Modeling promiscuity based on *in vitro* safety pharmacology profiling data. *ChemMedChem* 2:874–880

85. Jamieson C, Moir EM, Rankovic Z, Wishart G (2006) Medicinal chemistry of hERG optimizations: highlights and hang-ups. *J Med Chem* 49:5029–5046
86. Fischer H, Kansy M, Bur D (2000) CAFCA: a novel tool for the calculation of amphiphilic properties of charged drug molecules. *Chimia* 54:640–645
87. Clark J, Perrin DD (1964) Prediction of the strengths of organic bases. *Q Rev Chem Soc* 18:295–320
88. Morgenthaler M, Schweizer E, Hoffmann-Röder A, Benini F, Martin RE, Jaeschke G, Wagner B, Fischer H, Bendels S, Zimmerli D, Scheider J, Diederich F, Kansy M, Müller K (2007) Predicting and tuning physicochemical properties in lead optimization: amine basicities. *ChemMedChem* 2:1100–1115
89. Bruice PY (1984) Relative reactivity of amines and oxyanions toward proton abstraction from nitroethane. Electrostatic effects and the reactivity-selectivity principle. *J Am Chem Soc* 106:5959–5964
90. Trepka RD, Harrington JK, Belisle JW (1974) Acidities and partition coefficients of fluoro-methanesulfonamides. *J Org Chem* 39:1094–1098
91. Dean JA (1999) Lange's handbook of chemistry, 15th edn. McGraw-Hill, New York
92. Hansch C, Leo A, Taft RW (1991) A survey of Hammett substituent constants and resonance field parameters. *Chem Rev* 91:165c–195c
93. Taagepera M, Summerhays KD, Hehre WJ, Topsom RD, Pross A, Radom L, Taft RW (1981) Analysis of the acidities of 3- and 4-substituted pyridinium and anilinium ions. *J Org Chem* 46:891–903
94. Schlosser M (1998) Parametrization of substituents: effects of fluorine and other heteroatoms on OH, NH, and CH acidities. *Angew Chem Int Ed* 110:1496–1513
95. Olsen J, Seiler P, Wagner B, Fischer H, Tschopp T, Obst-Sander U, Banner DW, Kansy M, Muller K, Diederich F (2004) A fluorine scan of the phenylamidinium needle of tricyclic thrombin inhibitors: effects of fluorine substitution on pKa and binding affinity and evidence for intermolecular C-F CN interactions. *Org Biomol Chem* 2:1339–1352
96. Michalik L, Auwerx J, Berger JP, Chatterjee VK, Glass CG, Gonzalez FJ, Grimaldi PA, Kadowaki T, Lazar MA, O'Rahilly S, Palmer CAN, Plutzky J, Reddy JK, Spiegelman BM, Staels B, Wahli W (2006) International Union of Pharmacology. LXI. Peroxisome proliferator-activated receptors. *Pharmacol Rev* 58:726–741
97. Ciocoiu CC, Ravna AW, Sylte I, Rustan AC, Hansen TV (2011) Synthesis, molecular modeling studies and biological evaluation of fluorine substituted analogs of GW 501516. *Bioorg Med Chem* 19:6982–6988
98. Ishikawa M, Hashimoto Y (2011) Improvement in aqueous solubility in small molecule drug discovery programs by disruption of molecular planarity and symmetry. *J Med Chem* 54:1539–1554
99. Black WC, Bayly CI, Davis DE, Desmarais S, Falgueyret J-P, Léger S, Li CS, Massé F, McKay DJ, Palmer JT, Percival MD, Robichaud J, Tsou N, Zamboni R (2005) Trifluoroethylamines as amide isosteres in inhibitors of cathepsin K. *Bioorg Med Chem Lett* 15:4741–4744
100. Herrero S, Suárez-Gea ML, Suárez-Gea ML, González-Muñiz R, García-López MT, Herranz R, Ballaz S, Barber A, Fortuño A, Del Río J (1997) Pseudopeptide CCK-4 analogues incorporating the $\Psi[\text{CH}(\text{CN})\text{NH}$ peptide bond surrogate. *Bioorg Med Chem Lett* 855–860
101. Kirsch P (2004) Modern fluoroorganic chemistry, synthesis, reactivity applications. Wiley-VCH, Weinheim
102. Wipf P, Mo T, Geib SJ, Caridha D, Dow GS, Gerena L, Roncal N, Milner EE (2009) Synthesis and biological evaluation of the first pentafluorosulfanyl analogs of mefloquine. *Org Biomol Chem* 7:4163–4165
103. Welch JT, Lim DS (2007) The synthesis and biological activity of pentafluorosulfanyl analogs of fluoxetine, fenfluramine, and norfenfluramine. *Bioorg Med Chem* 15:6659–6666
104. Altomonte S, Zanda M (2012) Synthetic chemistry and biological activity of pentafluorosulphanyl (SF5) organic molecules. *J Fluor Chem* 143:57–93

105. Gujjar R, El Mazouni F, White KL, White J, Creason S, Shackelford DM, Deng X, Charman WN, Bathurst I, Burrows J, Floyd DM, Matthews D, Buckner FS, Charman SA, Phillips MA, Rathod PK (2011) Lead optimization of aryl and aralkyl amine-based triazolopyrimidine inhibitors of plasmodium falciparum dihydroorotate dehydrogenase with antimalarial activity in mice. *J Med Chem* 54:3935–3949
106. Smith DH, Waterbeemd H, Walker DK (2001) Pharmacokinetics and metabolism in drug design, methods and principles in medicinal chemistry, vol 13. Wiley-VCH, Weinheim
107. Barnette WE (1984) The synthesis and biology of fluorinated prostacyclins. *CRC Crit Rev Biochem* 15:201–235
108. Heek M, France CF, Compton DS, McLeod RL, Yumibe NP, Alton KB, Sybertz EJ, Davies HR Jr (1997) In vivo metabolism-based discovery of a potent cholesterol absorption inhibitor, SCH58235, in the rat and rhesus monkey through the identification of the active metabolites of SCH48461. *J Pharmacol Exp Ther* 283:157–163
109. Clader JW (2004) The discovery of ezetimibe: a view from outside the receptor. *J Med Chem* 47:1–9
110. Penning TD, Talley JJ, Bertenshaw SR, Carter JS, Collins PW, Docter S, Graneto MJ, Lee LF, Malecha JW, Miyashiro JM, Rogers RS, Rogier DJ, Yu SS, Anderson GD, Burton EG, Cogburn EG, Gregory SA, Koboldt CM, Perkins WE, Seibert K, Veenhuizen AW, Zhang AW, Isaakson PC (1997) Synthesis and biological evaluation of the 1,5-diarylpyrazole class of cyclooxygenase-2 inhibitors: identification of 4-[5-(4-methylphenyl)-3-(trifluoromethyl)-1*H*-pyrazol-1-yl]benzenesulfonamide (SC-58635, celecoxib). *J Med Chem* 40:1347–1365
111. Rosenblum SB, Huynh T, Afonso A, Davis HR Jr, Yumibe N, Clader JW, Burnett DA (1998) Discovery of 1-(4-fluorophenyl)-(3*R*)-[3-(4-fluorophenyl)-(3*S*)-hydroxypropyl]-(4*S*)-(4-hydroxyphenyl)-2-azetidinone (SCH 58235): a designed, potent, orally active inhibitor of cholesterol absorption. *J Med Chem* 41:973–980
112. St Jean Jr DJ, Fotsch C (2012) Mitigating heterocycle metabolism in drug discovery. *J Med Chem* 55:6002–6020
113. Wan Z-K, Chenail E, Xiang J, Li H-Q, Ipek M, Bard J, Svenson K, Mansour TS, Xu X, Suri V, Hahm S, Xing Y, Johnson CE, Li X, Qadri A, Panza D, Perreault M, Tobin JF, Saiah E (2009) Efficacious 11 β -hydroxysteroid dehydrogenase type I inhibitors in the diet-induced obesity mouse model. *J Med Chem* 52:5449–5461
114. Pierson PD, Fettes A, Freichel C, Gatti-McArthur S, Hertel C, Huwyler J, Mohr P, Nakagawa T, Nettekoven M, Plancher JM, Raab S, Richter H, Roche O, Rodríguez Sarmiento RM, Schmitt M, Schuler F, Takahashi T, Taylor S, Ullmer C, Wiegand R (2009) 5-Hydroxyindole-2-carboxylic acid amides: novel histamine-3 receptor inverse agonists for the treatment of obesity. *J Med Chem* 52:3855–3868
115. Seibert K, Zhang Y, Leahy K, Hauser S, Masferrer J, Perkins W, Lee L, Isakson P (1994) Pharmacological and biochemical demonstration of the role of cyclooxygenase 2 in inflammation and pain. *Proc Natl Acad Sci U S A* 91:12013–12017
116. Park BK, Kitteringham NR, O'Neill PM (2001) Metabolism of fluorine-containing drugs. *Annu Rev Pharmacol Toxicol* 41:443–470
117. Koerts J, Soffers AE, Vervoort J, De Jager A, Rietjens IM (1998) Occurrence of the NIH shift upon the cytochrome P450-catalyzed in vivo and in vitro aromatic ring hydroxylation of fluorobenzenes. *Chem Res Toxicol* 11:503–512
118. Dear GJ, Ismail IM, Mutch PJ, Plumb RS, Davies LS (2000) Urinary metabolites of a novel quinoxaline non-nucleoside reverse transcriptase inhibitor in rabbit, mouse and human: identification of fluorine NIH shift metabolites using NMR and tandem MS. *Xenobiotica* 30:407–426
119. Boguslavsky V, Bebecchi M, Morris AJ, Jhon DY, Rhee SG, McLaughlin S (1994) Effect of monolayer surface pressure on the activities of phosphoinositide-specific phospholipase C- β .1, - γ .1, and δ 1. *Biochemistry* 33:3032–3037
120. Hanakam F, Gerisch G, Lotz S, Alt T, Seelig A (1996) Binding of hisactophilin I and II to lipid membranes is controlled by a pH-dependent myristoyl–histidine switch. *Biochemistry* 35:11036–11044

121. Fischer H, Gottschlich R, Seelig A (1998) Blood-brain barrier permeation: molecular parameters governing passive diffusion. *J Membr Biol* 165:201–211
122. Lennamas H, Abrahamsson B (2005) The use of biopharmaceutical classification of drugs in drug discovery and development: current status and future extensions. *J Pharm Pharmacol* 57:273–285
123. Smart B (2001) Fluorine substituent effects (on bioactivity). *J Fluor Chem* 109:3–11
124. Jacobs RT, Bernstein PR, Cronk LA, Vacek EP, Newcomb LF, Aharony D, Buckner CK, Kusner EJ (1994) Synthesis, structure-activity relationships, and pharmacological evaluation of a series of fluorinated 3-benzyl-5-indolecarboxamides: identification of 4-[[5-[[[(2*R*)-2-methyl-4,4,4-trifluorobutyl]carbonyl]-1-methylindol-3-yl]methyl]-3-methoxy-N-[(2-methylphenyl)sulfonyl]benzamide, a potent, orally active antagonist of leukotrienes D₄ and E₄. *J Med Chem* 37:1282–1297
125. The Caco-2 cell line, derived from a human colorectal carcinoma, has become an established in vitro model for the prediction of drug absorption across the human intestine. When cultured on semi-permeable membranes, Caco-2 cells differentiate into a highly functionalized epithelial barrier with remarkable morphological and biochemical similarity to the small intestinal columnar epithelium. The membrane transport properties of novel compounds can thereby be assessed using these differentiated cell monolayers. The apparent permeability coefficients (P_{app}) obtained from Caco-2 cell transport studies have been shown to correlate to human intestinal absorption. Irvine JD, Takahashi L, Lockhart K, Cheong J, Tolan JW, Selick HE, Grove JR, (1999) MDCK (Madin–Darby canine kidney) cells: a tool for membrane permeability screening. *J Pharm Sci* 88:23–33
126. Pinto DJ, Orwat MJ, Wang S, Fevig JM, Quan ML, Amparo E, Cacciola J, Rossi KA, Alexander RS, Smallwood AM, Luetzgen JM, Liang L, Aungst BJ, Wright MR, Knabb RM, Wong PC, Wexler RR, Lam PY (2001) Discovery of 1-[3-(aminomethyl)phenyl]-N-[3-fluoro-2'-(methylsulfonyl)-[1,1'-biphenyl]-4-yl]-3-(trifluoromethyl)-1*H*-pyrazole-5-carboxamide (DPC423), a highly potent, selective, and orally bioavailable inhibitor of blood coagulation factor Xa. *J Med Chem* 44:566–578
127. Shimizu H, Yamasaki T, Yoneda Y, Muro F, Hamada T, Yasukochi T, Tanaka S, Toki T, Yokoyama M, Morishita K, Iimura S (2011) Discovery of imidazo[1,2-*b*]pyridazines as IKK β inhibitors. Part 3: Exploration of effective compounds in arthritis models. *Bioorg Med Chem Lett* 21:4550–4555 and refs therein
128. PAMPA: Parallel Artificial Membrane Permeability Assay is a method which determines the permeability of substances from a donor compartment, through a lipid-infused artificial membrane into an acceptor compartment. PAMPA models regularly exhibit a high degree of correlation with permeation across a variety of barriers including Caco-2 cultures, the GI tract, blood-brain barriers and skin
129. Carosati E, Sciabola S, Cruciani G (2004) Hydrogen-bonding interactions of covalently bonded fluorine atoms: from crystallographic data to a new angular function in the GRID force field. *J Med Chem* 47:5114–5125
130. Pfeleiderer T, Waldner I, Bertagnolli H, Tödheide K, Fischer HE (2000) The structure of liquid and supercritical deuterium fluoride from neutron scattering and using high-pressure techniques. *J Chem Phys* 113:3690–3696
131. Barbarich TJ, Rithner CD, Miller SM, Anderson OP, Strauss SH (1999) Significant inter- and intra-molecular O-H...F-C hydrogen-bonding. *J Am Chem Soc* 121:4280–4281
132. Murray-Rust P, Stallings WC, Monti CT, Preston RK, Glusker JP (1983) Intermolecular interactions of the C-F Bond: the crystallographic environment of fluorinated carboxylic acids and related structures. *J Am Chem Soc* 105:3206–3214
133. Scerba MT, Leavitt CM, Diener ME, DeBlase AF, Guasco TL, Siegler MA, Bair N, Johnson MA, Lectka T (2011) NH+–F hydrogen-bonding in a fluorinated “Proton Sponge” derivative: integration of solution, solid-state, gas-phase, and computational studies. *J Org Chem* 76:7975–7984
134. Prakash GKS, Wang F, Rahm M, Shen J, Ni C, Haiges R, Olah GA (2011) On the nature of C-H...F-C interactions in hindered CF₃-C(sp³) bond rotations. *Angew Chem Int Ed* 50:11761–11764

135. Chopra D (2012) Is organic fluorine really “not” polarizable? *Cryst Growth Des* 12:541–546
136. Dunitz JD (2004) Organic fluorine: odd man out. *ChemBioChem* 5:614–621
137. Cormanich RA, Freitas MP, Tormena CF, Rittner R (2012) The F...HO intramolecular hydrogen bond forming five-membered rings hardly appear in monocyclic organofluorine compounds. *RSC Adv* 2:4169–4174
138. Dunitz JD, Taylor R (1997) Organic fluorine hardly ever accepts hydrogen bonds. *Chem Eur J* 3:89–98
139. Fonseca TAO, Ramalho TC, Freitas MP (2012) F...HO intramolecular hydrogen bond as the main transmission mechanism for $^1\text{J}_{\text{F, H(O)}}$ coupling constant in 2'-fluoroflavonol. *Magn Reson Chem* 50:551–556
140. Cormanich RA, Moreira MA, Freitas MP, Ramalho TC, Anconi CPA, Rittner R, Contreras RH, Tormena CF (2011) $^1\text{J}_{\text{F, H}}$ coupling in 2-fluorophenol revisited: is intramolecular hydrogen bond responsible for this long-range coupling? *Magn Reson Chem* 49:763–767
141. Nolting DN, Nickels ML, Huo N, Pham W (2012) Molecular imaging probe development: a chemistry perspective. *Am J Nucl Med Mol Imaging* 2:273–306
142. Le Bars D (2006) Fluorine-18 and medical imaging: radiopharmaceuticals for positron emission tomography. *J Fluor Chem* 127:1488–1493
143. Miller PW, Long NJ, Vilar R, Gee AD (2008) Synthesis of ^{11}C , ^{18}F , ^{15}O and ^{13}N radiolabels for positron emission tomography. *Angew Chem Int Ed* 47:8998–9033
144. Ametamey SM, Honer M, Schubiger PA (2008) Molecular imaging with PET. *Chem Rev* 108:1501–1516
145. Pauwels EKJ, van der Klaauw AA, Corporaal T, Stokkel MPM (2002) Fluorine-18-radiolabeled pharmaceuticals for imaging with positron emission tomography, excluding [^{18}F]-fluorodeoxyglucose. *Drugs Future* 27:655–667
146. Daniels S, Farah M, Tohid S, Velanguparackel W, Westwel AD (2010) The role and future potential of fluorinated biomarkers in positron emission tomography. *Expert Opin Drug Discov* 5:291–304
147. Sharma S, Rodriguez AL, Conn PJ, Lindsley CW (2008) Synthesis and SAR of a mGluR5 allosteric partial antagonist lead: unexpected modulation of pharmacology with slight structural modifications to a 5-(phenylethynyl)pyrimidine scaffold. *Bioorg Med Chem Lett* 18:4098–4101
148. Sams AG, Mikkelsen AK, Brodbeck RMG, Pu X, Ritzén A (2011) Efficacy switching SAR of mGluR5 allosteric modulators: highly potent positive and negative modulators from one chemotype. *Bioorg Med Chem Lett* 21:3407–3410
149. Packiarajan M, Mazza Ferreira CG, Hong S-P, White AD, Chandrasena G, Pu X, Brodbeck RM, Robichaud AJ (2012) *N*-Aryl pyrrolidinonyl oxadiazoles as potent mGluR5 positive allosteric modulators. *Bioorg Med Chem Lett* 22:5658–5662
150. Packiarajan M, Mazza Ferreira CG, Hong S-P, White AD, Chandrasena G, Pu X, Brodbeck RM, Robichaud AJ (2012) Azetidinyloxadiazoles as potent mGluR5 positive allosteric modulators. *Bioorg Med Chem Lett* 22:6469–6474
151. Schirmmayer R, Wängler C, Schirmmayer E (2007) Recent developments and trends in ^{18}F -radiochemistry: syntheses and applications. *Mini Rev Org Chem* 4:317–329
152. Cai L, Lu S, Pike VW (2008) Chemistry with [^{18}F]-fluoride ion. *Eur J Org Chem* 2853–2873
153. Littich R, Scott PJH (2012) Novel strategies for fluorine-18 radiochemistry. *Angew Chem Int Ed* 51:1106–1109
154. Hollingworth C, Gouverneur V (2012) Transition metal catalysis and nucleophilic fluorination. *Chem Commun* 48:2929–2942
155. Prakash GKS, Chacko S (2008) Novel nucleophilic and electrophilic fluoroalkylation methods. *Curr Opin Drug Discov Dev* 11:793–802
156. Shimizu M, Hiyama T (2004) Modern synthetic methods for fluorine-substituted target molecules. *Angew Chem Int Ed* 44:214–231
157. Kirk KL (2008) Fluorination in medicinal chemistry: methods, strategies, and recent developments. *Org Proc Res Dev* 12:305–321

158. Furuya T, Kuttruff CA, Ritter T (2008) Carbon-fluorine bond formation. *Curr Opin Drug Discov Dev* 11:803–819
159. Pauwels EKJ (2001) ¹⁸F-Labeled fluorodeoxyglucose for PET imaging: the working mechanism and its clinical implication. *Drugs Future* 26:659–668
160. Gatley SJ, Volkow ND, Fowler JS, Ding Y-S, Logan J, Wang G-J, Gifford AN (2003) Positron emission tomography and its use to image the occupancy of drug binding sites. *Drug Dev Res* 59:194–207
161. Berridge MS, Heald DL, Lee Z (2003) Imaging studies of biodistribution and kinetics in drug development. *Drug Dev Res* 59:208–226
162. Hicks JW, Van Brocklin HF, Wilson AA, Houle S, Vasdev N (2010) Radiolabeled small molecule protein kinase inhibitors for imaging with PET or SPECT. *Molecules* 15:8260–8278
163. Badgaiyan RD (2011) Neurotransmitter imaging: basic concepts and future perspectives. *Curr Med Imaging Rev* 7:98–103
164. Jager PL, Chirakal R, Marriott CJ, Brouwers AH, Koopmans KP, Gulenchyn KY (2008) 6-L-¹⁸F-fluorodihydroxyphenylalanine PET in neuroendocrine tumors: basic aspects and emerging clinical applications. *J Nucl Med* 49:573–586
165. Minn H, Kauhanen S, Seppanen M, Nuutila P (2009) ¹⁸F-FDOPA: a multiple-target molecule. *J Nucl Med* 50:1915–1918
166. Garnett ES, Firnau G, Nahmias C (1983) Dopamine visualized in the basal ganglia of living man. *Nature* 305:137–138
167. DeJesus OT (2003) Positron-labeled DOPA analogs to image dopamine terminals. *Drug Dev Res* 59:249–260
168. Goodman MM, Kilts CD, Keil R, Shi B, Martarello L, Xing D, Votaw J, Ely TD, Lambert P, Owens MJ, Camp VM, Malveaux E, Hoffman JM (2000) ¹⁸F-Labeled FECNT: a selective radioligand for PET imaging of brain dopamine transporters. *Nucl Med Biol* 27:1–12
169. Davis MR, Votaw JR, Bremner JD, Byas-Smith MG, Faber TL, Voll RJ, Hoffman JM, Grafton ST, Kilts CD, Goodman MM (2003) Initial human PET imaging studies with the dopamine transporter ligand ¹⁸F-FECNT. *J Nucl Med* 44:855–861
170. Elsinga PH, Hatano K, Ishiwata K (2006) PET tracers for imaging of the dopaminergic system. *Curr Med Chem* 13:2139–2153
171. Chemel BR, Roth BL, Armbruster B, Watts VJ, Nichols DE (2006) WAY-100635 is a potent dopamine D4 receptor agonist. *Psychopharmacol* 188:244–251
172. Lang L, Jagoda E, Schmall B, Vuong B-K, Adams HR, Nelson DL, Carson RE, Eckelman WC (1999) Development of fluorine-18-labeled 5-HT_{1A} antagonists. *J Med Chem* 42:1576–1586
173. Lemaire C, Cantineau R, Marcel Guillaume M, Plenevaux A, Christiaens L (1991) Fluorine-18-altanserin: a radioligand for the study of serotonin receptors with PET: radiolabeling and in vivo biologic behavior in rats. *J Nucl Med* 32:2266–2272
174. Herth MM, Kramer V, Piel M, Palner M, Riss PJ, Knudsen GM, Roesch F (2009) Synthesis and in vitro affinities of various MDL 100907 derivatives as potential ¹⁸F-radioligands for 5-HT_{2A} receptor imaging with PET. *Bioorg Med Chem* 17:2989–3002
175. Gao Y, Kuwabara H, Spivak CE, Xiao Y, Kellar K, Ravert HT, Kumar A, Alexander M, Hilton J, Wong DF, Dannals RF, Horti AG (2008) Discovery of (–)-7-methyl-2-exo-[3'-(6-[¹⁸F] fluoropyridin-2-yl)-5'-pyridinyl]-7-azabicyclo[2.2.1]heptane, a radiolabeled antagonist for cerebral nicotinic acetylcholine receptor (α4β2-nAChR) with optimal positron emission tomography imaging properties. *J Med Chem* 51:4751–4764
176. Yang L, Rieves D, Ganley C (2012) Brain amyloid imaging – FDA approval of florbetapir F18 injection. *New Engl J Med* 367:885–887
177. Garber K (2012) First FDA-approved beta-amyloid diagnostic hits the market. *Nat Biotechnol* 30:575
178. Kung HF, Choi SR, Qu W, Zhang W, Skovronsky D (2010) ¹⁸F Stilbenes and styrylpyridines for PET imaging of Aβ plaques in Alzheimer's disease: a miniperspective. *J Med Chem* 53:933–941

179. Kung HF, Lee C-W, Zhuang ZP, Kung MP, Hou C, Plossl K (2001) Novel stilbenes as probes for amyloid plaques. *J Am Chem Soc* 123:12740–12741
180. Wang W, Oya S, Kung MP, Hou C, Maier DL, Kung HF (2005) F-18 stilbenes as PET imaging agents for detecting β -amyloid plaques in the brain. *J Med Chem* 48:5980–5988
181. Qu W, Kung MP, Hou C, Benedum TE, Kung HF (2007) Novel styrylpyridines as probes for SPECT imaging of amyloid plaques. *J Med Chem* 50:2157–2165
182. Zhang W, Oyas S, Kung MP, Hou C, Maier DL, Kung HF (2005) F-¹⁸F PEG stilbenes as PET imaging agents targeting A β aggregates in the brain. *Nucl Med Biol* 32:799–809
183. Zhang W, Kung MP, Oya S, Hou C, Kung HF (2007) ¹⁸F-labeled styrylpyridines as PET agents for amyloid plaque imaging. *Nucl Med Biol* 34:89–97
184. Stephenson KA, Chandra R, Zhuang Z-P, Hou C, Oya S, Kung M-P, Kung HF (2007) Fluoropegylated (FPEG): imaging agents targeting A β aggregates. *Bioconjug Chem* 18:238–246
185. Choi SR, Golding G, Zhuang Z, Zhang W, Lim N, Hefti F, Benedum TE, Kilbourn MR, Skovronsky D, Kung HF (2009) Preclinical properties of ¹⁸F-AV-45: a PET agent for A β plaques in the brain. *J Nucl Med* 50:1887–1894
186. Wong DF, Rosenberg PB, Zhou Y, Kumar A, Raymont V, Ravert HT, Dannals RF, Nandi A, Brašić JR, Ye W, Hilton J, Lyketsos C, Kung HF, Joshi AD, Skovronsky DM, Pontecorvo MJ (2010) In vivo imaging of amyloid deposition in Alzheimer's disease using the radioligand ¹⁸F-AV-45 (florbetapir F 18). *J Nucl Med* 51:913–920
187. Clark CM, Schneider JA, Bedell BJ, Beach TC, Bilker WB, Mintun MA, Pontecorvo MJ, Hefti F, Carpenter AP, Flitter ML, Krautkramer MJ, Kung HF, Coleman RE, Doraiswamy PM, Fleisher AS, Sabbagh MN, Sadowsky CH, Reiman PEM, Zehntner SP, Skovronsky DM (2011) Use of florbetapir-PET for imaging β -amyloid pathology. *J Am Med Assoc* 305:275–283
188. Fodero-Tavoletti MT, Brockschneider D, Villemagne VL, Martin L, Connor AR, Thiele A, Berndt M, McLean CA, Krause S, Rowe CC, Masters CL, Dinkelborg L, Dyrks T, Cappai R (2012) In vitro characterization of [¹⁸F]-florbetaben, an A β imaging radiotracer. *Nucl Med Biol* 39:1042–1048
189. Ashford JW, Rosen A, Adamson M, Bayley P, Sabri O, Furst A, Black SE, Weiner M, Barthel H, Sabri O (2011) Florbetaben to trace amyloid- β in the Alzheimer brain by means of PET. *J Alzheimer's Dis* 26(Suppl 3):117–121
190. Barthel H, Gertz H-J, Dresel S, Peters O, Bartenstein P, Buerger K, Hiemeyer F, Wittemer-Rump SM, Seibyl J, Reiningger C, Sabri O (2011) Cerebral amyloid- β PET with florbetaben (¹⁸F) in patients with Alzheimer's disease and healthy controls: a multicentre phase 2 diagnostic study. *Lancet Neurol* 10:424–435
191. Villemagne VL, Ong K, Mulligan RS, Holl G, Pejoska S, Jones G, O'Keefe G, Ackerman U, Tochon-Danguy H, Chan JG, Reiningger CB, Fels L, Putz B, Rohde B, Masters C, Rowe CC L (2011) Amyloid imaging with ¹⁸F-florbetaben in Alzheimer disease and other dementias. *J Nucl Med* 52:1210–1217
192. Nelissen N, van Laere K, Thurfjell L, Owenius R, Vandenbulcke M, Koole M, Bormans G, Brooks DJ, Vandenberghe R (2009) Phase 1 study of the Pittsburgh compound B derivative ¹⁸F-flutemetamol in healthy volunteers and patients with probable Alzheimer disease. *J Nucl Med* 50:1251–1259
193. Wong DF, Moghekar Abhay R, Rigamonti D, Brasic JR, Rousset O, Willis W, Buckley C, Smith A, Gok B, Sherwin P, Grachev ID (2013) An in vivo evaluation of cerebral cortical amyloid with ¹⁸F-flutemetamol using positron emission tomography compared with parietal biopsy samples in living normal pressure hydrocephalus patients. *Mol Imaging Biol* 15: 230–237
194. Vandenberghe R, Van Laere K, Ivanoiu A, Salmon E, Bastin C, Triau E, Hasselbalch S, Law I, Andersen A, Korner A, Minthon L, Garraux G, Nelissen N, Bormans G, Buckley C, Owenius R, Thurfjell L, Farrar G, Brooks DJ (2010) ¹⁸F-flutemetamol amyloid imaging in Alzheimer disease and mild cognitive impairment: a phase 2 trial. *Ann Neurol* 68:319–329
195. Cselenyi Z, Joehagen ME, Forsberg A, Halldin C, Julin P, Schou M, Johnstroem P, Varnaes K, Svensson S, Farde L (2012) Clinical validation of ¹⁸F-AZD4694, an amyloid- β -specific PET radioligand. *J Nucl Med* 53:415–424

196. Jureus A, Swahn B-M, Sandell J, Sandell J, Jeppsson F, Johnson AE, Johnstroem P, Neelissen JAM, Sunnemark D, Farde L, Svensson SPS (2010) Characterization of AZD4694, a novel fluorinated A β plaque neuroimaging PET radioligand. *J Neurochem* 114:784–794
197. Li Z, Conti PS (2010) Radiopharmaceutical chemistry for positron emission tomography. *Adv Drug Deliv Rev* 62:1031–1051
198. Riss PJ, Ferrari V, Brichard L, Burke P, Smith R, Aigbirhio FI (2012) Direct, nucleophilic radiosynthesis of [^{18}F]-trifluoroalkyl tosylates: improved labelling procedures. *Org Biomol Chem* 10:6980–6986
199. Moon BS, Kil HS, Park JH, Kim JS, Park J, Chi DY, Lee BC, Kim SE (2011) Facile aromatic radiofluorination of [^{18}F]-flumazenil from diaryliodonium salts with evaluation of their stability and selectivity. *Org Biomol Chem* 9:8346–8355
200. Lee E, Kamlet AS, Powers DC, Neumann CN, Boursalian GB, Furuya T, Choi DC, Hooker JM, Ritter T (2011) A fluoride-derived electrophilic late-stage fluorination reagent for PET imaging. *Science* 334:639–642
201. Liu W, Huang X, Cheng M-J, Nielsen RJ, Goddard WA III, Groves JT (2012) Oxidative aliphatic C-H fluorination with fluoride ion catalyzed by a manganese porphyrin. *Science* 337:1322–1325